T.C.

AYDIN ADNAN MENDERES UNIVERSITY

GRADUATE SCHOOL OF NATURAL AND APPLIED SCIENCES

MASTER'S PROGRAMME IN CIVIL ENGINEERING

DELAMINATION ANALYSIS OF CURVED LAMINATED GLASSES

SİMGE VURAL

MASTER'S THESIS

SUPERVISOR

Assoc. Prof. Dr. Ebru DURAL

AYDIN-2021

ACCEPTANCE AND APPROVAL

The thesis entitled "DELAMINATION ANALYSIS OF CURVED LAMINATED GLASSES" prepared by Simge VURAL, a student of the Department of Civil Engineering program at T.C. Aydın Adnan Menderes University, Graduate School of Natural and Applied Sciences, was accepted as Master's thesis by the jury below.

Date of Thesis Defence: 15/09/2021

Member : Assoc. Prof. Dr. Ebru DURAL   Aydın Adnan Menderes University
(T.D.)

Member : Assoc. Prof. Dr. Emre AKIN   Mersin University

Member : Asst. Prof. Dr. Gözde Başak   Aydın Adnan Menderes University
       ÖZTÜRK ÖZERAY

APPROVAL

This thesis was approved by the jury above in accordance with the relevant articles of the Aydin Adnan Menderes University Graduate Education and Examination Regulations and was approved on the ……………………………. by from the Board of Directors of the Graduate School of Science in the ……………………………. numbered decision.

Prof. Dr. Gönül AYDIN

Institute Director

ACKNOWLEDGEMENTS

I would like to thank my supervisor Ebru Dural for her support and guidance throughout the research. I would also like to thank my family for their understanding and support during my study.

TABLE OF CONTENTS

LIST OF SYMBOLS AND ABBREVATIONS

A_1, A_2 : Cross sectional area of upper and lower glass ply

b : Width of the beam

γ_I : Shear strain in the interlayer for curved beam

E : Modulus of elasticity of glass

$\varepsilon\,^i_m$: Membrane strain energy for the upper and lower ply

$\varepsilon\,^i_b$: Bending strain energy for the upper and lower ply

G : Shear modulus of interlayer

h_1, h_2 : Thicknesses of upper and lower arches, respectively

θ, r : Polar coordinates

I_1, I_2 : Moment of inertia of upper and lower glass arches

$N1, N2$: Circumferential forces in upper and lower glass arches, respectively

P : Point load applied to the center of the beam

q : Uniformly distributed load applied over the length of beam

Π :Total potential energy of the system

ρ : Poission ratio of the interlayer

t : Thickness of the interlayer

U : Total strain energy

$u1, u2$: Circumferential displacement for the upper and lower ply in the θ direction

U^1_m, U^2_m : The membrane strain energies of upper and lower glass layers, respectively

U^1_b, U^2_b :The bending strain energies of upper and lower glass layers, respectively

U_I :The shear strain energy of the PVB interlayer

V : Potential energy of applied loads

Ω : Load potential function

V̆ : Applied shear force

M̃ : Applied moment

LIST OF FIGURES

LIST OF TABLES

ÖZET

EĞRİSEL LAMİNE CAMLARIN DELAMİNASYON ANALİZİ

Vural S. Aydın Adnan Menderes Üniversitesi, Fen Bilimleri Enstitüsü, İnşaat Mühendisliği Bölümü, Yüksek Lisans Tezi, Aydın, 2021

Amaç: Bu tezin amacı farklı sınır koşullarına maruz kalan delamine olmuş eğrisel cam kirişlerin davranışını analiz etmektir.

Materyal ve Yöntem: Bu tezde cam kirişlerin başlangıçtaki delaminasyon durumu göz önünde bulundurarak matematiksel modellemesi ve sonlu elemanlar modellemesi yapılmıştır. Eğrisel lamine cam kirişlerin doğrusal olmayan davranışını çözümleyebilmek için minimum potansiyel enerji ilkeleri kullanılarak bir matematiksel model geliştirilmiş ve hakim denklemlerin çözümü tekrarlamalı çözüm yöntemi kullanılarak elde edilmiştir. Elde edilen doğrusal olmayan denklemleri sayısal olarak çözmek için bilgisayar programı geliştirilmiş elde edilen sonuçlar geliştirilen sonlu elemanlar modeli ile karşılaştırılmıştır ve sonuçlar grafikler halinde verilmiştir.

Bulgular: Delamine cam birimlerin nonlineer davranış gösterdiği gözlemlenmiştir. Sabit mesnetli merkez delemaniasyonlu kirişin basit mesnetli kirişe göre nonlineerlik seviyesi daha yüksektir. Farklı sınır koşullarında analizler yapılmış ve bunun sonucunda basit mesnetli kirişin sabit mesnetli kirişe göre daha fazla daha fazla gerilme ve deplasman değerine sahip olduğu görülmüştür. Ayrıca merkez delaminasyona sahip eğrisel kirişin davranışı lamine, katmanlı ve monolithik cam ile karşılaştırıldığında katmanlı cama daha yakın bir davranış gösterdiği gözlemlenmiştir ve delamine olmuş camın gücünün delamine olmuş bölgenin lokasyonuna göre değişiklik gösterdiği gözlemlenmiştir

Sonuç: Bu çalışmada delamine eğrisel cam kirişlerin davranışının delaminasyonun lokasyonuna ve farklı sınır koşullarına göre değişiklik gösterdiği saptanmıştır.

Anahtar Kelimeler: Lamine cam, Eğrisel kiriş, Delaminasyon, Doğrusal olmayan davranış.

ABSTRACT

DELAMINATION ANALYSIS OF CURVED LAMINATED GLASSES

Vural S. Aydın Adnan Menderes University, Graduate School of Natural and Applied Sciences, Civil Engineering Program, Master Thesis, Aydın, 2021

Objective: The purpose of this thesis is to analyze the behavior of delaminated curved laminated glass beams exposed to different boundary conditions**.**

Material and Methods: In this thesis, mathematical modeling and finite element modeling of glass beams have been made, considering the initial delamination state. In order to analyze the nonlinear behavior of curved laminated glass beams, a mathematical model has been developed using the minimum potential energy principles and the solution of the equations has been obtained by using the iterative solution method. A computer program was developed to solve the obtained nonlinear equations numerically, the results were compared with the developed finite element model and the results were given in graphics.

Results: It was observed that the delaminated glass units showed nonlinear behavior. The level of nonlinearity of the fixed supported central delaminated beam is higher than the simply supported beam. Analyzes were made in different boundary conditions and as a result, it was seen that the simply supported beam had more stress and deflection values than the fixed supported beam. In addition, the behavior of the curved beam with center delamination was observed to be closer to the layered glass compared to laminated, layered and monolithic glass, and it was observed that the strength of the delaminated glass varies according to the location of the delaminated region.

Conclusion: In this study, it was determined that the behavior of delaminated curved glass beams varies according to the location of the delamination and different boundary conditions**.**

Keywords: Laminated glass, Curved beam, Delamination, Nonlinear behavior

1. INTRODUCTION

Glass is a widely used material since ancient times. It is obtained by mixing and melting various raw materials, especially sand, soda, limestone, in certain ratios and properties, and passing them through various processes. The structure of the glasses consists of an irregular silicon network, and silico-soda-lime glass is often used to manufacture the glasses. There are four main processes in glass production. These four processes are batching, melting, fining and forming, respectively. While producing glass, the first three stages are applied for all glasses, but forming and the processes to be done afterward vary depending on which glass product we want to obtain. In the batching process, the right raw material mixes are selected. In this process, raw materials are selected according to chemistry, homogeneity, purity and particle size. The glass blend, which is a mixture of substances with certain properties and amounts, is then passed to the melting process. Glass furnaces are used in this process. Different products are obtained by using different furnaces. After this stage, the molten glass goes into the fining stage. The purpose of this process is to ensure that the glass is homogeneous in terms of temperature and composition and that there are no bubbles in the glass. After this stage, the forming process is started according to the desired glass type. Annealed, fully tempered, heat strengthened and laminated glasses are the most commonly used glass types.

Annealed glass is standard flat glass and has not been further treated. When broken, annealed glass breaks into large pieces. While producing float glass, after adjusting the raw material mixture in certain proportions, the mixture is melted at a temperature of about 1600 °C temperature and a thinning process is applied to eliminate the bubbles in it. The melt obtained is transferred to the tin pool after it reaches approximately 1100 °C temperature. By floating the glass on the tin pool, it is ensured that the two sides of the glass are flawless and parallel to each other. Rollers are used to produce glass in different thicknesses. Thanks to the rollers placed on the upper part of the glass, it is ensured that the glass reaches the desired thickness. Then, the temperature of the glass is reduced in a controlled manner and in the cooling section, the stresses on the glass are eliminated. Then the glass is formed to the desired dimensions.

The production of tempered glass occurs by heating the annealed glass homogeneously up to 700°C and cooling the annealed glass abruptly by exposing it to cold air jets. The purpose of this process is to create a parabolic residual stress field with tensile stresses in the core of the glass and compressive stresses on the surfaces, thus tempered glass is four to five times stronger than annealed glass of the same size and thickness against impact. When the tempered glass is broken, all the energy stored in it is released at the same time, and the tempered glass is broken into small pieces, which are harmless, so full tempered glass is also called as safety glass.

Heat strengthened glass and tempered glass are produced in a similar way. The only difference in this process is the low cooling rate. The lower the cooling rate, the lower the resulting residual stress. Its tensile strength is lower than that of fully tempered glass. Glass fragments larger than tempered glass are formed when broken.

With the development of laminated glass, glass has started to be used at every point of our lives. Although laminated glass is a widely used material today, its use in the architecture and construction industry has just become widespread.

Laminated glass is a material formed by bonding two or more layers of glass together with an elastomeric interlayer. While producing laminated glass, float glass of desired color and thickness is cut to the appropriate size. If curved laminated glass is desired to be obtained, the inner and outer glasses are placed on top of each other and bent in the bending furnaces. The softening temperature of the glass is 600 degrees, and the glass that reaches this temperature is put into a circular mold and given a curved shape with the help of gravity. After the glasses, which have been bent into shape, are cleaned with special cleaning systems, 0.76 mm thick PVB (polyvinyl butyral) is placed between the inner and outer layers. The interlayer is usually polyvinyl butyral, and the PVB interlayer can also be put as 0.38, 0.76 and 1.52 mm. Autoclave is performed after the air between the PVB and the glass is sucked. The glasses and PVB are autoclaved at a pressure of 12-14 bar and a temperature of 150 ^{0}C for a certain period of time. PVB (Polyvinyl Butyral) is a preferred material as a binder interlayer in laminated glasses. The PVB interlayer holds the laminated glass together in case of breakage and prevents it from breaking. Due to this feature of laminated glass, it has become a preferred material in car windshields and aircraft manufacturing. Laminated glass is a preferred glass coating material in architecture due to its protection from bomb explosions,

hurricanes and natural disasters. In addition, the properties such as ultraviolet screening, sound control and solar energy control make laminated glass a preferred material.
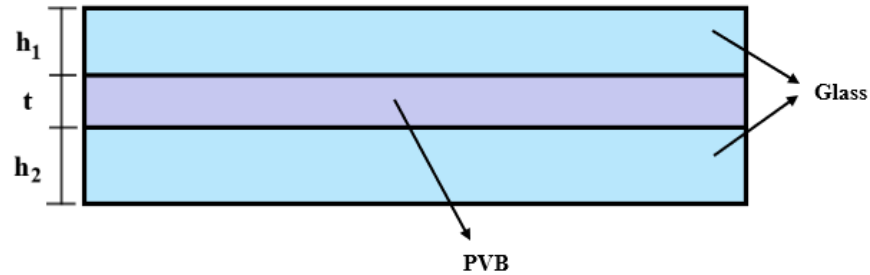
Figure 1.1.1 Laminated glass

Two different types of materials are used in laminated glass. These materials are PVB and glass, so the behavior of laminated glass becomes quite complex. The reason for this problem is likely to be that the modulus of elasticity of the glass is 10^4 times greater than the polyvinyl butyral material. In addition, the laminated glass unit is very thin and it shows large displacement even under its own weight. These properties complicate the behavior of the laminated glass.

Glass, could be used as layered, laminated and monolithic in structural applications. Layered glass consists of two glasses stacked on top of each other and there is no friction between them. Stress distribution is symmetrical on each ply around separate neutral axes for simple support beam. Plane sections do not remain plane in this situation and the centers of curvature of the two plies being different. Since the layers act independently in fix supported layered system beams, they enter the non-linear region before equivalent monolithic systems.

Monolithic glass consists of a single pane of glass. The stress distribution of a simply supported monolithic glass beam is the distribution of a single beam symmetrical about the neutral axis of the entire section, and the plane sections remain plane.

Laminated glass is a material created by connecting two glasses with an interlayer. The stress distribution in the cross section of the laminated glass is formed by the two triangular stress distributions in the layered glass and the constant coupling stress of the interlayer. The triangular stress distribution of the laminated glass is symmetrical about the neutral axes of

3

each layer. The shear modulus of the interlayer affects the value of the coupling stress, and when pressure is applied to the upper layer, the coupling stress is compressive in the upper layer, while it creates tensile stress in the lower layer.
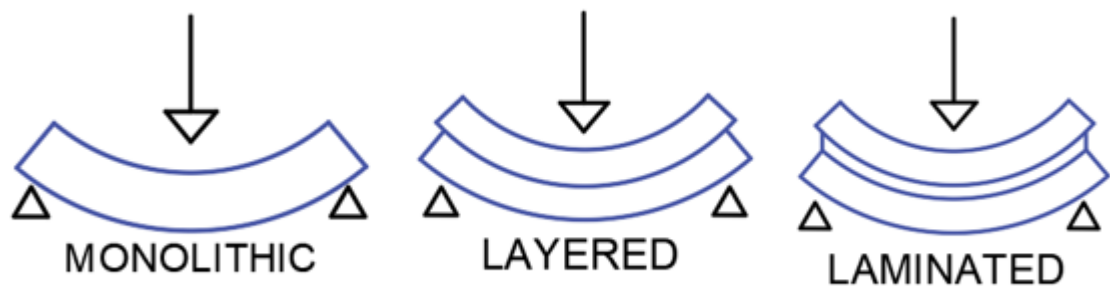
Figure 1.1.2 Monolithic, layered and laminated units.

Delamination is a big problem in laminated glass. Delamination can be defined as breaking the bond between the interlayer and glass layers in a laminated glass unit. The biggest cause of delamination in laminated glass is the faults in the production process. Edge delamination, Worm or Finger delamination, Sunburst delamination, and Snowflake delamination are types of delamination. These delaminations occur due to possible reasons in the process. These issues can lead to many problems in laminated glass, for example, it can reduce the load-carrying capacity of the structure and greatly affect the structural stiffness of the structure. PVB is a substance that can undergo structural changes. If it is exposed to moisture, it swells, and when dries again it shrinks. The high seasonal and daily temperature differences also cause edge delamination.

The environmental conditions in which laminated materials are stored are also effective for the formation of delamination. For example, PVB tends to soften when the temperature of the substance is high. The softening material causes a decrease in stickiness and separation from the layers. It is more common in the days after autoclaving. Worm or Finger delamination is caused by the stress of laminate material or weak PVB-Glass bond. Gaps in the glass in worm delamination can increase the risk of delamination. The adhesive bond

4

around the delamination may be weak. Glass endpoints are region under stress. High internal pressure points are regions with spherical bubbles. It can release the pressure by spreading this pressure from the spherical bubble to a large area. As a result of relieving this pressure, worm delamination occurs. The moisture of the PVB material, the ionized particles deposited on the glass, the continuation of the process at high temperature during the autoclave process, the fluidization of the laminated material in a very hot environment and the gap ratio between the glasses are effective in the bond between PVB and glass. Sunburst delamination is caused by excess air or volatile matter trapped in the material. If the Sunburst delamination is not complete, a small amount of air is released by pressing on the delamination area, which is ineffective if there is excess air in the delamination.

Delamination includes differences according to where it occurs. The type of delamination that takes place between PVB and glass and occurs between the normal and softer PVB layer. This delamination is seen as a circular area where the bond between PVB-Glass is insufficient and occurs near the midpoints of the material. Snowflake delamination appears as white bubles in areas where the bond between PVB-Glass has failed and has the appearance of circular sunburst around this white area. This delamination area is distinguished by its intense white color. It is formed by the continuous exposure of laminated glass to water and moisture. Due to the weak bonding structure of PVB due to water, its adhesive property is lost. Water turns a certain point of the PVB substance into an intense white color. PVB material can be dried and made transparent again, but if the water content is above 1.5%, the white color becomes dominant and has a non-recyclable structure.

2. LITERATURE REVIEW

Over the past years there has been a dramatic increase in studies about laminated glass due to increasing use. In literature, a great deal of research has been carried out to predict the mechanical response of laminated glass units.

2.1 Studies About Laminated Glass Conducted By Hooper

Hooper (1973) has done important research on laminated glass beams. Hooper aimed to get an idea about the basic behavior of architectural laminated glass in bending. Therefore, Hooper conducted theoretical and experimental studies on the effect of laminated glass beam on bending at four points. Using the Laplace transform, Hooper solved the equations related to the axial force and bending moment applied to one of the layers and determined three impact factors (K1, K2, K3) depending on the axial force. The impact factors K1, K2, K3 are proportional to the axial force at one of the plies, the shear strain at the intermediate layer, and the central deflection.

Hooper carried out two types of experiments, each involved loading the laminated beam in standard four-point bending. Numerous small strain-measuring beams were quickly loaded through a universal testing machine, deflections in the center of the beams were measured, and strain gauge measurements allowed the bending stresses to be determined across the laminated section. In the other experiment, tests were carried out for the beams subjected to continuous load at various ambient temperatures and the central deflection of each beam was measured at intervals throughout the test. As a result, Hooper found that the degree of connection between the two glass layers depends on the shear modulus of the intermediate layer, and they observed that the shear modulus of interlayer is a function of both the ambient temperature and the loading time.

2.2 Experimental Studies Conducted By Chen Et Al.

Chen et al. (2014), explained a simple cracking initiation law related to cracks in laminated glass plates. In the experiment laminated glass bonded by PVB interlayer was used for impact test. PVB's Young modulus 0.1 GPa, Poison's ratio 0.49, density 1100 kg/m^3; for glass: Youngs's modulus 70 GPa, Poison's ratio 0.22 and density 2500 kg/m^3). In the experiment in-plane dimension of plate specimen is 200mm x 150mm. Thickness of glass on both side is 2 mm and PVB thickness changes 0.76 to 3.04. All laminated glass prepared with 10 bar pressure and 120 °C temperature.

Impact tests were performed using a drop-weight test platform. The experiment was carried out with different loading speeds. The experiment was supported by a high-speed photographic system. This system allowed the in-situ quantification and recording of dynamic crack growth. This system with a maximum of 1000 mm and a drop weight of 2 kg was used to provide the impact energy required for the dynamic loading test.

As a result of these experiments, it was observed that the cracks formed in the two glass plates were completely matched even though they spread at different times, and it was observed that the cracks first started in the supported glass layer. The crack propagation time of the sample containing a PVB interlayer with a thickness of 0.76 mm is 70 μs at a loading speed of 3.7 m/s. The maximum crack velocity obtained in this period was obtained at 1150 m/s. The resumption of radial cracks in the loaded layer occurred at approximately 700 μs. This study showed that when PVB laminated glasses are subjected to impact loading, the glass layer will always begin to break before the loaded layer, and the final structure of radial cracks on both sides will be completely similar even if they propagated at different times.

2.3 Experimental Study Conducted By Serafinavicius Et Al. (2013)

The long-term behavior of the structural glass plates was explained by the four-point bending test with different interlayers and long-term experiments at different temperatures. In these experiments, 6mm thick soda-lime-silica glasses were used and DuPont's SentryGlas (SG), Polyvinyl Butyral (PVB) and Ethylene Vinyl Acetate (EVA) were preferred as different

intermediate layers. The dimensions of the samples used in the experiment were selected as 360 mm width, 1100 mm length and 1.52 mm lamination film thickness.

Based on European Standards, long-term tests were applied to specimens bent at four points, and these tests were conducted in a climate chamber. Temperatures (+20 °C, + 30°C , + 40°C) were selected according to the technical specifications of the climate chamber. The samples were left under constant loading for the entire 72-hour test period, and the constant loading was determined as 0.512 kN for all the same glass plates. Three different measurement methods were used in this experiment. These are Mid-Span Deviations, Volatile Displacements and Longitudinal Strains.

PVB glass plate deflection values increasing from average 7 mm at + 20°C up to 8 mm at + 40°C. At + 20°C, the EVA laminate is almost not bent, but at + 30°C, a very small deflection difference is noted. Maximum deviation values were obtained at + 40 ° C and observed to be equal to 3.5 mm. Looking at the Measured Volatile Displacements, the average displacement values of the PVB interlayer increased from (0.12 mm at + 20°C) to (0.15 mm at + 40°C). There is no slippage in the SG interlayer during 24 hours loading time at 20°C. It starts to slide at + 30°C and the value is below 0.001mm. At + 40°C temperature, the slip value does not exceed 0.005 mm. The structure of the EVA material between the laminated glass changes according to the temperature. Therefore, small slip occurs in laminated glass. Considering the results of the measured longitudinal strains, it was observed that the highest value was in PVB. Tensile stress average values are from 17 MPa at + 20°C until 20 MPa at + 40°C. Tensile stress values for EVA laminated glass plates measured approximately: 12 MPa at + 20°C, 13 MPa at + 30°C, 14 MPa at + 40°C, and tensile stresses of SG laminated glass plates measured 9 MPa at + 20°C, 10 MPa at + 30°C and 11 MPa at + 40°C.

2.4 Mathematical Model Developed By Dural (2016)

In this research, Dural developed a mathematical model for the initial delaminated laminated glass beams. Dural revised the three nonlinear field differential equations, developed by Aşık and Tezcan according to the delamination state. In order to obtain the field differential equations, variational principles were used and the equations were obtained by minimizing the potential energy unit. It is assumed that the intermediate layer does not have

significant bending strength and only transmits shear stresses and each glass beam in a laminated glass unit has its own neutral axis, bending and axial strain energies resulting from lateral and axial deformations, but the intermediate layer has only shear strain energy.

Finite difference method was used to transform the obtained differential equations into algebraic equations. Matrix forms were created to obtain the horizontal and in-plane displacements. Dural conducted experiments to verify the assumptions of the developed mathematical model. Three-point bending tests were applied to determine the bending, stresses for various loading conditions to define the mechanical behavior of the delaminated glass beam unit. The experiment was applied to two different beam types as, simply and fixed supported. In the experimental study, delamination was applied in three different proportion.

Delaminated specimens were produced as 15 cm, 20 cm and 40 cm symmetrically in the midpoint of the unit. The results obtained from these experiments were compared with the results obtained from the mathematical model.

2.5 Finite Element Model Developed By Peng et al.'s

Peng et al. (2013) discussed the situation when the pedestrian's head hit the windshield of the car during the accident. They examine the mechanical behavior of the car window using finite element model. Behavior of windshield of the car is analyzed for different connection types and mesh sizes (5 mm and 10 mm).

Peng et al. set up a finite element model for five windshields, and LS-DYNA code was taken into account when setting up this model. These are;

M-L-G= Glass-PVB- Glass

G-P-S= Glass-PVB- Share

G-P-T= Glass-PVB-Tied

G-P-G-S= Glass-PVB-Glass-Share

G-P-G-T= Glass-PVB-Glass-Tied

FE model has been validated by EEVC tests. A standard EEVC head impactor which has a weight of 4.8 kg, was used in the test. This impactor was pushed in the middle of the

glass and at a right angle to the corner points. The speed of the head form in this test is 11.1 m / s. In addition, In order to see how the breakage stresses of the glass affects the behavior of the glass, a parametric study was carried out using 5 different breaking stresses. Clamped boundary condition is used to further validate the FE model. As a result of the FE model, experiments and parametric studies, it was seen that the G-P-T (5 mm mesh) model for car windshields is the best model to represent a car windshield. 50 MPa failure stress was the best predictor of head form acceleration and cracks in glass. The data in this study will be enlightening at the design stage in order to prevent damage to the victim in case of head hitting the vehicle windows.

2.6 Experimental Study Conducted By Ibekwe et al.'s

A study was carried out by Ibekwe et al. (2007) to investigate the impact and post-impact response of laminated beams at low temperatures. For this test, 50 samples were used and these samples were cooled in the environmental chamber using liquefied nitrogen. The impact test was conducted at 20 ° C, 10 ° C, 0 ° C, -10 ° C, and -20° C , and all coupons were struck at a speed of 2 m \ s and energy of 12.8 J. After the impact test, compression tests were carried out at the same temperature and analyzed using TEST STAR II software.

As a result of the tests, it was observed that samples affected at lower temperatures had more impact damage than those at high temperatures, and cross-ply laminates were observed to provide more impact resistance. The residual compressive buckling strength and elastic modulus increase as the temperature decreases until -10 ° C. When the temperature reaches -20 ° C, both the compression buckling strength and elastic modulus decrease. Also, cross-ply laminates have higher resistance to impact damage at lower velocity than unidirectional laminates. It has been observed that unidirectional laminates have higher residual buckling strength than ply laminates at operating temperatures.

2.7 Experimental Study Conducted By Centalles et al.'s

A double-lap shear test was carried out on laminated glass specimens after different aging tests by Centalles et al. (2020). In this study four different types of interlayer material were used. These four materials are SentryGlas, Saflex DG-41, EVASAFE and PVB BG-R20. Four material double lap shear specimens were exposed to four different aging tests. These four different tests; humidity test, two different UV radiation tests and thermal cycling test followed by double-lap shear test.

While performing the thermal cycling test, the samples were forced to temperatures ranging from 30 °C to 60 °C and to remain constant for 30 minutes at both ends. 3.2 °C/min forced convection cooling was used as the heating rate. This procedure 100 times applied.

For the humidity test, the samples were placed over a bath for two weeks, a closed container has an air temperature of 50 °C and a relative humidity of 100%. While performing the UV radiation tests, a series of double-lap shear samples were subjected to a radiation source with similar properties to solar radiation at a temperature of 45 ± 5°C. Two different waiting times have been suggested in previous studies, so Centalles et al. used two different waiting times to compare the results. Tested exposure times of 265 hours and 2000 hours. After the whole aging test, the double-lap shear test was applied.

As a result, in this study, it was noticed that the stress distribution was not homogeneous in the glass layers, it was observed that the stress in the outer glass layers was higher in the region where the bond with the central layers ended. In addition, stress peaks were formed at the upper and lower edges of the stress distribution on the bond surface at the junction between the interlayer and the glass, and it was noticed that these stress peaks were not in a homogeneous structure. The results also show that, according to the mechanical properties of the interlayer material and the level of adhesion to the glass; This indicates that there may be a loss of adhesion between the glass and the interlayer, and sometimes subsequent glass breakage. The results also showed that the selected test materials and sample structure were sufficient to compare the response with different interlayer materials when exposed to different aging conditions.

2.8 Mathematical Model Developed By Aşık et al.'s

Aşık et al. (2014) conducted a study on curved laminated glasses. A mathematical model was developed using large deflection theory, since laminated glass exhibits nonlinear behavior and its thickness is very small compared to its width and length. Aşık et al. obtained a potential energy equation by using the membrane, bending, shear and potential energies of glasses and shear strain values of the interlayer. The field equations were obtained by taking the first derivatives of this equation according to the circumferential and radial displacements, and then the finite element model was created by considering the fix end case to verify the results in the mathematical model. They used ABAQUS version 6.7-1 for the finite element model. In addition, an experimental study was conducted for validation and comparison. Three point bending tests were performed and the results were compared.

2.9 Various studies about the delamination of laminated glass

Some investigations about behavior of delaminated glass units are available in the literature.

Gadelrab (1996) studied the effect of delamination on the natural frequencies of laminated composite beams. He stated that in the case of delamination, the dynamic feature of the structure in the laminated beam changes and it provides flexibility. Therefore, in this research, the finite element method is used to understand the effect of the length of the delamination and the starting point from the ending condition on natural frequencies. It has been obtained that the delamination condition reduces the natural frequencies for the laminated composite beam as it provides a local flexibility in the beam. As a result of this study, it was found that the increase in the delaminated region ratio increased the percentage deviation in the natural frequencies of the system, and it was revealed that the diagnoses and detection of delamination can be made non-destructively by monitoring the frequency changes thanks to the typical frequency tables obtained in this study.

Saponara et al. (2006) used experiments and finite element (FE) models to investigate crack growth from delamination in composite materials. Load-displacement response and crack length were monitored by performing tests on cross-ply graphite/epoxy specimens under static conditions, and tests were performed using an Instron 8501 hydraulic testing machine with a 100 KN load cell. It was observed that the crack distribution and strain values in the FE model matched the values obtained in the experiment.

Geleta (2018) et al. investigated the delamination behavior of L-shaped laminated composites numerically and experimentally by using cohesive region modeling. Two configurations of L-shaped curved laminates were used in this study. One of these configurations (Config-I) was taken from the reference where the numerical result was verified and the other (Config-II) was from the reference where both the experiment and analysis were made. Adhesive elements are placed in the interlayers to represent the delamination formation, and different types of loading are applied to the laminated composite models, allowing the delamination to be opened and cut.

As a result of the loadings, different delamination propagation patterns were obtained for the two cases, it was determined that the arm lengths were different. Also, in Config-II with long arm length, the delamination remained in the curved part, in Config-I, since the arm is shorter, it was determined that the arm lengths were a different way spread.

Jaśkowiec (2015) has produced three-dimensional modeling of the failure of a delaminated laminated glass. The extended finite element method (XFEM) is used to perform the numerical modelling. XFEM was used to model the PVB interlayer. The modeling described in this study is explained with an example. Young's modulus of PVB changes a lot with temperature, so in this example Young is taken as $3.73x10^3$ and $0.373x10^3$ values. Young's modulus of PVB is inversely proportional to temperature. While its value decreases as the temperature increases, it starts to increase when the temperature is decreased, but in this study, the behavior of PVB is predicted with a linear model.

According to Zubillaga et al. (2015) conducted an experimental study to observe the formation of matrix cracking and delamination. Tensile tests were carried out with universal servo-hydraulics. While performing these experiments, five different lay-ups were selected and an idea about the initiation and propagation of the damage was obtained. Four of the selected samples were delaminated due to matrix crack growth. Only in one of them the failure continued only with the matrix crack. The values obtained from the experiments were

compared with the failure criteria made by the authors before and it was observed that they matched the experimental data as a result.

The main aim of the present study is to investigate the effect of delamination on bending behavior, boundary conditions and strength factor of laminated glass curved beams. To this end, a mathematical model based on minimization of potential energy is developed to investigate the effect of delamination in the case of simply and fixed supported curved beams, and nonlinear finite element analyses are performed to investigate the effect of nonlinearity in the case of simple end beams. The effect of various parameters like delamination size, boundary conditions are investigate by the help of the mathematical model.

3. MATERIAL AND METHOD

3.1 Mathematical Modelling

In this thesis, the mathematical model developed by Dural (2011) to observe the bending behavior of laminated glass arches, has been modified for the delamination state. A mathematical model was developed to analyze behavior of delaminated glass arches. In this model, minimum potential energy principle is used. With the minimum potential energy principle, the total potential energy is minimized. The total potential energy of the laminated glass system is defined as the sum of the bending energy of the glasses, the membrane energy of the glasses, the energy resulting from the shear deformation of the interlayer, and the force potential energies. The first variation of the total potential energy of the unit with respect to the circumferential and radial displacements give the field differential equations and boundary conditions. Figure 3.1.1 shows the laminated glass curved beam and its parts.
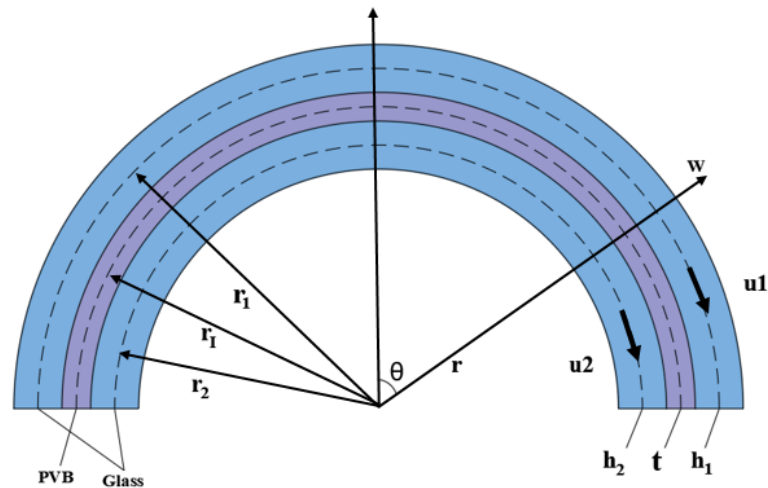

Figure 3.1.1 Laminated glass curved beam

In order to develop mathematical modeling, some assumptions have been made about the glass unit:

1. The beam material is considered to be completely homogeneous and isotropic.

2. The beam material obeys Hooke's law and is completely elastic.

3. Shear deformation is ignored since the glass beam has a small thickness.

4. Plane sections that are initially normal to the mid-surface are considered to remain plane and normal to the mid-surface during bending for each glass ply, but not for one unit.

5. In-plane displacement derivatives are too small for nonlinear behavior so the high powers of the in-plane displacement derivatives and their products are ignored.

6. In the laminated glass unit, the layers are very thin so it is assumed that the radial deflection in the cross section does not change.

And the following assumptions have been made for the interlayer:

1. It is assumed that the plane section before deformation remains plane after deformation.

2. Material is isotropic and homogenous.

3. The material obeys Hooke's law and it is elastic.

4. It is assumed that no slippage occurs between the adjacent faces of the layers and the intermediate layer.

5. A simplification is provided by assuming linear shear strains instead of finite strains.

6. PVB has negligible compression in the transverse direction and only transmits shear.

In line with the assumptions made for the glass and interlayer, the total potential energy equation for the system was obtained as follows:

$$\pi = U_m^1 + U_b^1 + U_m^2 + U_b^2 + U_I + \Omega \tag{3.1}$$

U_m^1, U_m^2 = The membrane strain energies of upper and lower glass layers, respectively

U_b^1, U_b^2 = The bending strain energies of upper and lower glass layers, respectively

U_I = The shear strain energy of the PVB interlayer

Ω = The potential energy due to the applied loads

$$\pi = \sum_{i=1}^{2}\left\{\int_V \frac{1}{2}E\left(\varepsilon_m^i\right)^2 dV + \int_V \frac{1}{2}E\left(\varepsilon_b^i\right)^2 dV\right\} + \int_V \frac{1}{2}G\left(\gamma_i\right)^2 dV - \int_0^S qw ds \qquad (3.2)$$

where ;

$$\varepsilon_m^1 = \frac{u_{1\theta} + w}{r_1} + \frac{1}{2}\left(\frac{w_\theta}{r_1}\right)^2 \qquad\qquad \varepsilon_m^2 = \frac{u_{2\theta} + w}{r_2} + \frac{1}{2}\left(\frac{w_\theta}{r_2}\right)^2$$

$$\varepsilon_b^1 = -z\frac{w_{\theta\theta}}{r_1^2} \qquad\qquad \varepsilon_b^2 = -z\frac{w_{\theta\theta}}{r_2^2}$$

The deformed and undeformed geometry shown in Figure 3.1.2 below is used to obtain the shear strain of the unit.
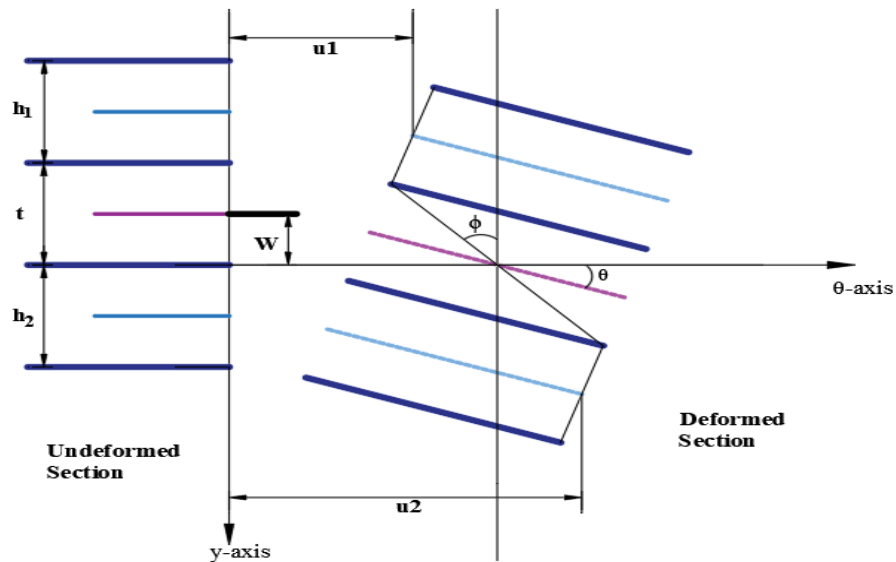

Figure 3.1.2 Deformed and undeformed parts of the laminated glass section

And shear strain for the pvb interlayer is:

$$\gamma_I = \frac{u_1 - u_2 - \left(\dfrac{1}{r_1} \dfrac{h_1}{2} + \dfrac{1}{r_2} \dfrac{h_2}{2} + \dfrac{t}{r_1} \right) \dfrac{dw}{d\theta}}{t}$$

The total potential energy of the system in extended form is:

$$\pi = \sum_{i=2}^{2} \left\{ \int_V \frac{1}{2} E \left(\frac{u_{i\theta} + w}{r_i} + \frac{1}{2} \left(\frac{w_\theta}{r_i} \right)^2 \right)^2 dV + \int_V \frac{1}{2} E \left(-z \frac{w_{\theta\theta}}{r_i^2} \right)^2 dV \right\} + \tag{3.3}$$

$$\int_V \frac{1}{2} G \left(\frac{u_1 - u_2 - \left(\dfrac{1}{r_1} \dfrac{h_1}{2} + \dfrac{1}{r_2} \dfrac{h_2}{2} + \dfrac{t}{r_1} \right) \dfrac{dw}{d\theta}}{t} \right)^2 dV - \int_0^S qw ds$$

Variation of total potential energy with respect to circumferential displacement of upper and lower glass arces (u_1, u_2) and radial displacements (w) gives the field differential equation.

$$\delta\pi[u_1] = 0$$
$$\delta\pi[u_2] = 0$$
$$\delta\pi[w] = 0$$

Three nonlinear field differential equations and boundary conditions for curved laminated glass beam are obtained as follows:

$$\frac{d}{d\theta^2} \left(EI \frac{d^2 w}{d\theta^2} \right) - \frac{d}{d\theta} \left(\left(\frac{N_1}{r_1} + \frac{N_2}{r_2} \right) \frac{dw}{d\theta} \right) + (N_1 + N_2) + \tag{3.4}$$

$$Gbr_1 \left(\frac{1}{r_1} \frac{h_1}{2} + \frac{1}{r_2} \frac{h_2}{2} + \frac{t}{r_1} \right) \frac{d\gamma_I}{d\theta} - qr_1 = 0$$

$$\frac{dN_1}{d\theta} - Gbr_I \gamma_I = 0 \qquad (3.5)$$

$$\frac{dN_2}{d\theta} - Gbr_I \gamma_I = 0 \qquad (3.6)$$

where;

$$N_1 = EA_1 \left(\frac{u_{1\theta} + w}{r_1} + \frac{1}{2r_1^2} W_\theta^2 \right) \tag{3.7}$$

$$N_2 = EA_2 \left(\frac{u_{2\theta} + w}{r_2} + \frac{1}{2r_2^2} W_\theta^2 \right) \tag{3.8}$$

$$I = I_1 + I_2 \text{ and } \qquad I_1 = \frac{bh_1^3}{12r_1^3} \ , \quad I_2 = \frac{bh_2^3}{12r_2^3}$$

The field equations extended form are given below in terms of displacement;

$$EI \frac{d^4 w}{d\theta^4} - \frac{Gbr_I}{t} \left(\frac{1}{r_1}\frac{h_1}{2} + \frac{1}{r_2}\frac{h_2}{2} + \frac{t}{r_1} \right)^2 (w_{\theta\theta}) = qr_1 + \frac{EA_1}{r_1} \left(\frac{u_{1\theta\theta} + w_\theta}{r_1} + \frac{w_{\theta\theta} w_\theta}{r_1^2} \right) w_\theta$$

$$+ \frac{EA_1}{r_1} \left(\frac{u_{1\theta} + w}{r_1} + \frac{w_\theta^2}{2r_1^2} \right)(w_{\theta\theta} - 1) + \frac{EA_2}{r_2} \left(\frac{u_{2\theta\theta} + w_\theta}{r_2} + \frac{w_{\theta\theta} w_\theta}{r_2^2} \right) w_\theta \tag{3.9}$$

$$+ \frac{EA_2}{r_2} \left(\frac{u_{2\theta} + w}{r_2} + \frac{w_\theta^2}{2r_2^2} \right)(w_{\theta\theta} - 1) - \frac{Gbr_I}{t} \left(\frac{1}{r_1}\frac{h_1}{2} + \frac{1}{r_2}\frac{h_2}{2} + \frac{t}{r_1} \right) \left(\frac{du_1}{d\theta} - \frac{du_2}{d\theta} \right)$$

$$\frac{EA_1}{r_1} (u_{1\theta\theta}) - \frac{Gbr_I}{t} u_1 = \frac{EA_1}{r_1} (w_\theta) \left(1 + \frac{1}{r_1} w_{\theta\theta} \right) \tag{3.10}$$

$$+ \frac{Gbr_I}{t} \left(-u_2 - \left(\frac{1}{r_1}\frac{h_1}{2} + \frac{1}{r_2}\frac{h_2}{2} + \frac{t}{r_1} \right) \frac{dw}{d\theta} \right)$$

$$\frac{EA_2}{r_2} (u_{1\theta\theta}) - \frac{Gbr_I}{t} u_2 = \frac{EA_2}{r_2} (w_\theta) \left(1 + \frac{1}{r_2} w_{\theta\theta} \right) \tag{3.11}$$

$$- \frac{Gbr_I}{t} \left(u_1 - \left(\frac{1}{r_1}\frac{h_1}{2} + \frac{1}{r_2}\frac{h_2}{2} + \frac{t}{r_1} \right) \frac{dw}{d\theta} \right)$$

The following steps can be followed to obtain the boundary conditions of the curved beam:

At $\theta = \theta_1$ and $\theta = \theta_2$ (at supports of curved unit) for Equation (3.4)

$$-\frac{d}{d\theta}\left(EI\frac{d^2}{d\theta^2}\right)+\left(N_1+N_2\right)\frac{dw}{d\theta}$$

$$-\frac{Gbr_I}{t}\left(\frac{1}{r_1}\frac{h_1}{2}+\frac{1}{r_2}\frac{h_2}{2}+\frac{t}{r_1}\right)\left[u_1-u_2-\left(\frac{1}{r_1}\frac{h_1}{2}+\frac{1}{r_2}\frac{h_2}{2}+\frac{t}{r_1}\right)\frac{dw}{d\theta}\right]=\breve{V}$$

or radial deflection w is previously assigned,

$$-EI\frac{d^2w}{d\theta^2}=\breve{M}\text{ or }\frac{dw}{d\theta}\text{ is previously assigned,}$$

For Equation (3.5) and (3.6)

$$\frac{EA_1}{r_1}\left(\frac{u_{1\theta}+w}{r_1}\right)+\frac{w_\theta^2}{2r_1^2}=\breve{N}_1\text{ or }u_1\text{ is previously assigned },$$

$$\frac{EA_2}{r_2}\left(\frac{u_{2\theta}+w}{r_2}\right)+\frac{w_\theta^2}{2r_2^2}=\breve{N}_2\text{ or }u_2\text{ is previously assigned },$$

$\breve{V}=$ Applied shear force

$\breve{M}=$ Applied moment

$\breve{N}_1$ and $\breve{N}_2=$ Applied axial for upper and lower glass arches

If no force is applied to a simply supported curved beam at its ends, the boundary conditions are as follows:

At $\theta=\theta_1$ and $\theta=\theta_2$ (at supports) $\qquad w=0$ and $\dfrac{d^2w}{d\theta^2}=0$

$$u_1=0\quad\text{and }u_2=0$$

If no force is applied to fixed supported curved beam at its ends, the boundary conditions are as follows:

At $\theta=\theta_1$ and $\theta=\theta_2$ (at the supports) $\qquad w=0$ and $\dfrac{dw}{d\theta}=0$

$$u_1=0\quad\text{and }u_2=0$$

In order to model the response of delaminated glass curved beam it is thought that there is no bond between the glass layer and the PVB interlayer in the delaminated areas of the

glass beam. It is accepted that the glass and PVB layers are separated from each other. In derivation of the above field equations, it is assumed that the PVB interlayer only transfers shear force. Therefore, the field equations are rearranged by taking the shear force transmitted by the interlayer in the delaminated areas of the beam as zero. Terms with shear modulus are ignored. While the above field equations are valid for the undelaminated regions. The field equations for the delaminated areas are obtained as follows.

$$EI \frac{d^4 w}{d\theta^4} = qr_1 + \frac{EA_1}{r_1} \left(\frac{u_{1_{\theta\theta}} + w_\theta}{r_1} + \frac{w_{\theta\theta} w_\theta}{r_1^2} \right) w_\theta$$

$$+ \frac{EA_1}{r_1} \left(\frac{u_{1_{\theta+w}}}{r_1} + \frac{w_\theta^2}{2r_1^2} \right) (w_{\theta\theta} - 1) + \frac{EA_2}{r_2} \left(\frac{u_{2_{\theta\theta}} + w_\theta}{r_2} + \frac{w_{\theta\theta} w_\theta}{r_2^2} \right) w_\theta \qquad (3.12)$$

$$+ \frac{EA_2}{r_2} \left(\frac{u_{2_\theta} + w}{r_2} + \frac{w_\theta^2}{2r_2^2} \right) (w_{\theta\theta} - 1)$$

$$\frac{EA_1}{r_1} \left(u_{1_{\theta\theta}} \right) = \frac{EA_1}{r_1} \left(w_\theta \right) \left(1 + \frac{1}{r_1} w_{\theta\theta} \right) \qquad (3.13)$$

$$\frac{EA_2}{r_2} \left(u_{2_{\theta\theta}} \right) = \frac{EA_2}{r_2} \left(w_\theta \right) \left(1 + \frac{1}{r_2} w_{\theta\theta} \right) \qquad (3.14)$$

Solution of three nonlinear differential equations (3.12), (3.13), (3.14), which governs the behavior using analytical methods is quite difficult, so the numerical finite difference method (FDM) was used to solve these equations. The solution procedure was suggested by Dural (2011) for laminated glass curved beam. The central finite difference method is used to convert nonlinear differential equations into algebraic equations and to write them in matrix form. All the nonlinear terms in the field equations have been collected on the right. An iterative procedure is used in the solution because the equations are connected and not linear. Since smaller load increment results in easier convergence, the applied load is usually increased slowly in nonlinear analysis. For each applied load-step, the solver needs to be iterated until convergence criteria is met. When the converged results are obtained the results are written and the next step is undertaken.

The equations are modified at the boundaries of the unit in accordance with the geometry and the applied load is evaluated in small increments for convergence. The field equations become as follows:

21

[A]{w}=RHS

[A]= Qui-diagonal matrix that only the elements belonging to five diagonals are stored as vectors.(Coefficient matrix for radial displacement)

RHS= Right hand side vector which includes applied load and other terms that are calculated at every discrete point on the right hand side of Equation (3.9) and (3.12).

{w}= Radial displacement vector

For the radial deflection;

$\Delta\theta$ = Finite difference mesh size

n= Number of subdivision in the θ direction

Since the radial deflection is known as zero at the supports, the end points are not included in the solution process to reduce the total number of equations. The central finite difference method is applied to the field equations and equations are obtained in algebraic form. The central finite difference expression of the field equation for radial deflection in the domain for curved laminated glass without delamination:

$$Aw_{i-2} + Bw_{i-1} + Cw_i + Dw_{I+1} + Ew_{i+2} = RHS_i \quad \text{for i=2, 3, ..., n-1} \tag{3.15}$$

where the coefficient of the matrix and the right end side (RHS) vector in extended form:

$$A = E = 1$$

$$B = D = -4 - \frac{Gbr_I}{Elt}\left(\frac{1}{r_1}\frac{h_1}{2} + \frac{1}{r_2}\frac{h_2}{2} + \frac{t}{r_I}\right)^2 (\Delta\theta)^2,$$

$$C = 6 + \frac{(\Delta\theta)^4}{EI}\left(\frac{Ebh_1}{r_1} + \frac{Ebh_1}{r_1}\right) + 2\frac{Gbr_I}{Elt}\left(\frac{1}{r_1}\frac{h_1}{2} + \frac{1}{r_2}\frac{h_2}{2} + \frac{t}{r_I}\right)^2 (\Delta\theta)^2,$$

$$RHS = \frac{EA_2}{r_I}w_\theta\left(\frac{u_{1_{\theta\theta}} + w_\theta}{r_1} + \frac{w_{\theta\theta}w_\theta}{r_1^2}\right) + \frac{EA_1}{r_1}\left(\frac{u_{1_\theta} + w}{r_1} + \frac{w_\theta^2}{2r_1^2}\right)(w_{\theta\theta} - 1)$$

$$+ \frac{EA_2}{r_2}w_\theta\left(\frac{u_{2_{\theta\theta}} + w_\theta}{r_2} + \frac{w_{\theta\theta}w_\theta}{r_2^2}\right) + \frac{EA_2}{r_2}\left(\frac{u_{2_\theta} + w}{r_2} + \frac{w_\theta^2}{2r_2^2}\right)(w_{\theta\theta} - 1)$$

$$- \frac{Gbr_I}{t}\left(\frac{1}{r_1}\frac{h_1}{2} + \frac{1}{r_2}\frac{h_2}{2} + \frac{t}{r_I}\right)\left(\frac{du_1}{d\theta} - \frac{du_2}{d\theta}\right) + qr_1$$

Since the field equations are modified in the delaminated regions of laminated unit the coefficient of algebraic equations need to be modified. The central finite difference expression of the required field equation for the radial deflection in the field for the delaminated curved glass beam is done as follows.

$$A = E = 1$$
$$B = D = -4$$
$$C = 6 + \frac{(\Delta\theta)^4}{EI}\left(\frac{Ebh_1}{r_1} + \frac{Ebh_1}{r_1}\right),$$

$$RHS = \frac{EA_2}{r_1}w_\theta\left(\frac{u_{1_{\theta\theta}} + w_\theta}{r_1} + \frac{w_{\theta\theta}w_\theta}{r_1^2}\right) + \frac{EA_1}{r_1}\left(\frac{u_{1_\theta} + w}{r_1} + \frac{w_\theta^2}{2r_1^2}\right)(w_{\theta\theta} - 1)$$

$$+ \frac{EA_2}{r_2}w_\theta\left(\frac{u_{2_{\theta\theta}} + w_\theta}{r_2} + \frac{w_{\theta\theta}w_\theta}{r_2^2}\right) + \frac{EA_2}{r_2}\left(\frac{u_{2_\theta} + w}{r_2} + \frac{w_\theta^2}{2r_2^2}\right)(w_{\theta\theta} - 1) + qr_1$$

The iterative solution procedure for each load increment is done by following the steps below:

1) Make an initial assumption for displacements w, u_1 and u_2,

2) Calculate right hand side vector <u>RHS</u>,

3) Obtain $w(i)$ from Eq (3.15)

4) Apply successive over relaxation method to obtain convergent results

$$w(i) = \alpha w(i) + (1-\alpha)w_o(i),$$

5) Conduct error analysis $\dfrac{\sum_i |w(i) - w_o(i)|}{(num * w_{max})} \leq tol$ then stop,

6) Calculate the right hand side of the equation (3.13) and obtain circumferential displacement of upper glass unit u_1,

7) Calculate the right hand side of the equation (3.14) and obtain circumferential displacement of lower glass unit u_2,

8) go to step 2,

In this procedure α is the under relaxation parameter. It is calculated by interpolation regarding the nondimensional maximum deflection $2*w(\max)/(h_1+h_2)$ as a result of numerical experiment, and $w_0(i)$ is the radial deflection calculated in the previous step.

3.2 Finite Element Investigation

The model developed by Dural (2011) for laminated glass arch was verified by Aşık et al. (2014) performing three point bending test. The specimens they used were curved laminated glass with 5+1.52+5 mm thicknesses. The radius of upper glass was 1000 mm while lower glass and interlayer radius were 993.48 mm and 996.74 mm, respectively. Comparison of the maximum stress values are given by Aşık et al. (2014). They observed a good correlation between the experimental results and the developed mathematical model.

In the current study Dural's model was modified for delaminated glass units. To confirm the assumptions of the developed mathematical model, the finite element model is compared with the result. This comparison was made according to the case of simply supported beams. The two-dimensional model for finite element modeling was created and solved with Abaqus version 6.13. The load was chosen as the concentrated load and applied at the midpoint of the beam. While constructing the mesh, 4-node bilinear plane stress quadrilateral elements (CPS4R) were used. The dimensions of the laminated glass model were chosen as 100 mm width and 1 m outer glass radius. In addition, the thickness was determined as 5 mm outer and inner glass, 0.76 mm PVB interlayer. All physical properties of curved laminated glass beam are shows in Table 3.1. The Young's modulus of the glass was taken as 72 Gpa, while the Poisson's ratio was taken as 0.25. For the intermediate layer, Shear modulus is taken as 1000 kPa, while Poisson's ratio is 0.29. Horizontal and vertical degrees of freedom of all nodes at both ends of the beam were set to zero in order to create the simple supported boundary condition in the model. To perform large deformation analysis, "nonlinear geometry option" was selected. The glass layers and PVB interlayer were bounded using tie option. In order to represent the effect of delamination in the delaminated areas of the specimen the layers were not bounded each other and constraints were not created. Figure 3.2.1 shows the representation of constraints. Delamination is arranged at the center of unit as 0.5 m. A view of deformed and undeformed unit is presented in Figure 3.2.2.
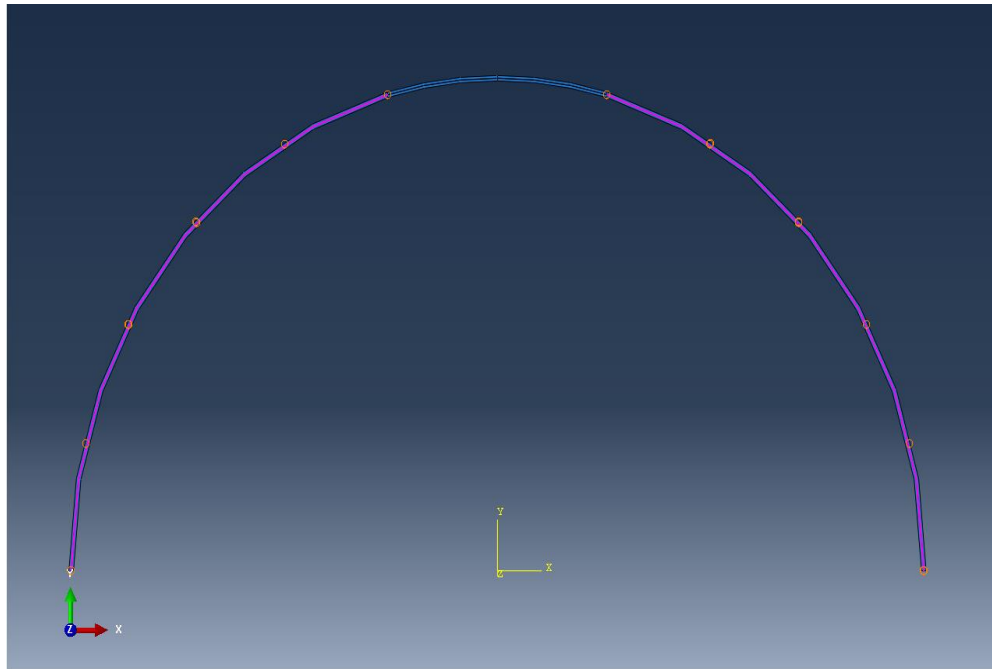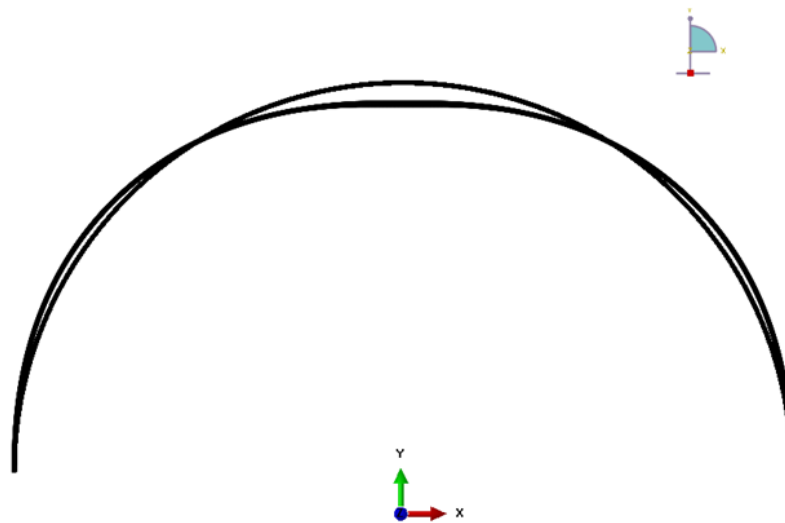
Figure 3.2.1 Representation of constraints.

Figure 3.2.2 Deformed and undeformed unit.

The physical properties of curved beam used in the finite element model are given in table 3.2.1.

	Modulus		Dimensions (mm)			
	E	G	Width	Radius	Thickness	Arc Length
Glass 1	72 Gpa	28.8 GPa	100	1000	5	3140
PVB	3000 kPa	1000 kPa	100	997.12	0.76	3140
Glass 2	72 GPa	28.8 GPa	100	994.24	5	3140

Table 3.2.1 Modulus and dimensions of laminated glass curved beam

Table 3.2.2 and Figures 3.2.3 and 3.2.4 below give a comparison of deflections and stresses for a simply supported laminated glass beam.

	Stress (MPa)			Displacement (m)		
Point Load (N)	Finite Element Model	Mathematical Model	Error	Finite Element Model	Mathematical Model	Error
0.00	0.00	0.00	0.00	0.00	0.00	0.00
100.00	15.80	17.77	11.11	4.92	5.55	11.40
200.00	30.92	34.76	11.05	9.48	10.68	11.21
300.00	46.19	51.05	9.52	13.71	15.43	11.17
400.00	61.07	66.73	8.48	17.60	19.87	11.41
500.00	74.98	81.85	8.39	21.30	24.01	11.29
600.00	87.27	96.46	9.53	24.88	27.90	10.83
700.00	99.97	110.63	9.63	29.03	31.57	8.03
800.00	113.60	124.37	8.66	33.16	35.02	5.32
900.00	127.80	137.73	7.21	37.28	38.30	2.65
1000.00	142.00	150.74	5.80	41.37	41.40	0.07
1100.00	156.10	163.42	4.48	45.43	44.35	-2.44
1200.00	170.30	175.80	3.13	49.45	47.15	-4.87
1300.00	184.50	187.89	1.80	53.44	49.83	-7.24
1400.00	198.70	199.71	0.51	57.38	52.39	-9.53
1500.00	212.90	212.43	-0.22	60.06	54.83	-9.53
1600.00	227.10	222.62	-2.01	62.09	57.18	-8.59
1700.00	241.30	233.73	-3.24	64.66	59.42	-8.82
1800.00	255.50	244.64	-4.44	67.57	61.58	-9.73
1900.00	267.90	255.34	-4.92	70.01	63.65	-9.99
2000.00	283.90	265.86	-6.79	72.00	65.65	-9.68

Table 3.2.2 Comparison of stress and displacement values for the simply supported laminated curved beam

Looking at the graph obtained from the table, Figure 3.2.3, it is shows that the current model and the finite element model (FEM) give similar deflection values. The maximum error value, that is, the difference, was obtained as 11.11% for applied very small load and as the load is increasing error decreases. In the comparison made for the stress values in Figure 3.2.4, the maximum margin of error was obtained as 11.40%. As a result of the comparisons, no significant difference was observed. This result shows us that the model prepared to analyze the behavior of curved delaminated glass beams gives reliable results for the simply supported delaminated curved glass beam unit.
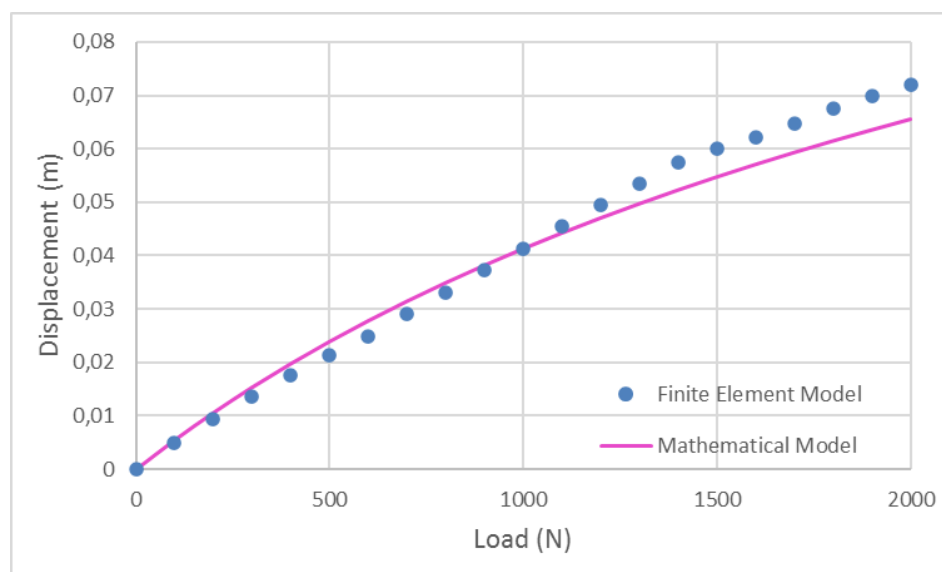
Figure 3.2.3 Central deflection values of the simply supported laminated glass curved beam
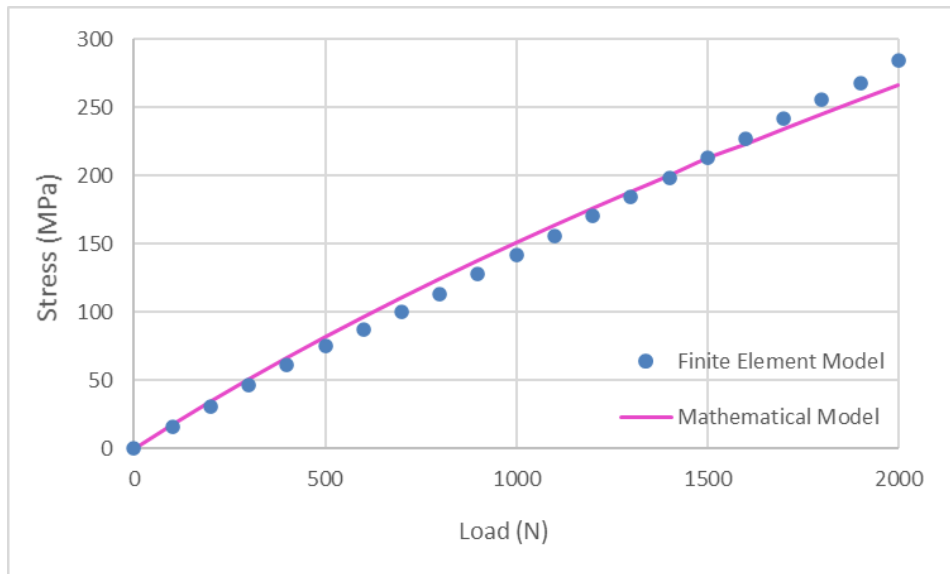
Figure 3.2.4 Maximum stress values of the simply supported laminated glass curved beam

4. RESULTS

4.1 Curved laminated glass beam subjected to simply supported boundary condition

Due to constant cross-sectional force, beams subjected to simply supported edge conditions shows linear behavior under loading, even at large deformations. Because of the free surface where the total cross sectional force is zero, membrane stresses don't developed at simply supported beam. For simple support it is easy to make comparisons for different geometries like, layered laminated and monolithic units thanks to the linear behavior.

The material and geometric properties of the curved glass beam unit, given in Figure 3.1, can be listed as follows. r_1=1 m, θ=3.14, h_1=h_2=5 mm, interlayer thickness t is equal to 0.76 mm, width of unit b=0.1 m, 1000 kPa, E=72× 10^6 kPa and concentrated load at the midpoint of the outer glass arch was accepted as P = 2 kN. To have a convergent sequence, the load was applied in 0.002 kN increments. It is very useful to use a variable SOR (successive over-relaxation) parameter to get a convergent solution so radial displacement w is interpolated by using SOR parameter α which changes with the ratio of $\dfrac{w_{max}}{h}$.

Arranging the boundary terms in the variational equations, boundary condition of simply supported beam are obtained as follows. Figure 4.1 shows pictorial representation of simply supported arch.

At $\theta = \theta_1$ and $\theta = \theta_2$ (at the left and right supports):

$$w = 0 \quad \text{and} \quad \frac{d^2 w}{d\theta^2} = 0$$

$$u_1 = 0 \text{ and } u_2 = 0$$

w=0

u1=0 $\quad \dfrac{d^2w}{d\theta^2}=0$

u2=0

w=0

u1=0 $\quad \dfrac{d^2w}{d\theta^2}=0$

u2=0
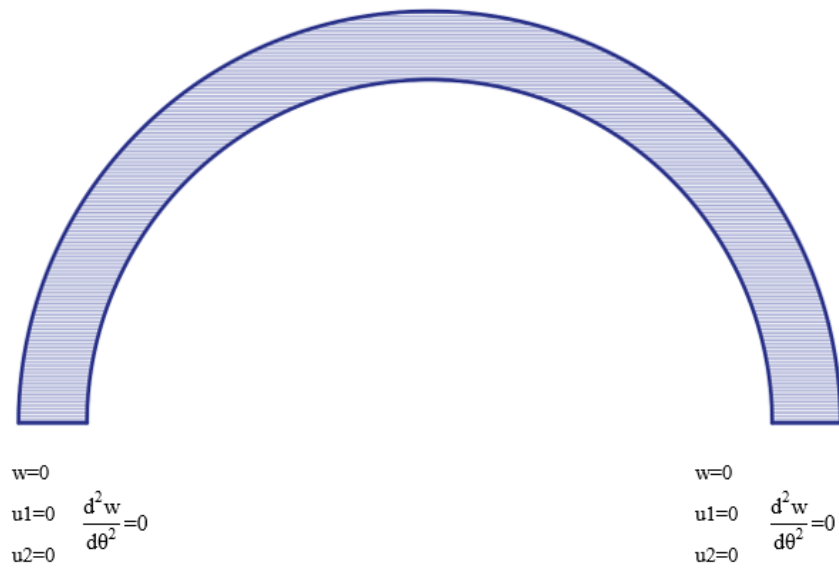
Figure 4.1.1 Representation of the boundary conditions of a simply supported curved beam on the figure.

In the numerical study that deals with the effect of the delamination location on the behavior of the curved laminated glass beam, delaminations are considered in three different locations. The size of delamination is 0.5 m. In the first specimen, Specimen 1, delamination occurs in the center of unit as 0.5 m. In the second specimen, Specimen 2, the delamination occurs at the edge of the unit as 0.5 m. In the third specimen, Specimen 3, the delamination occurs between 0.535-1.035 m far away from the left boundary. The location of delamination for each case is shown in Fig. 4.1.2.
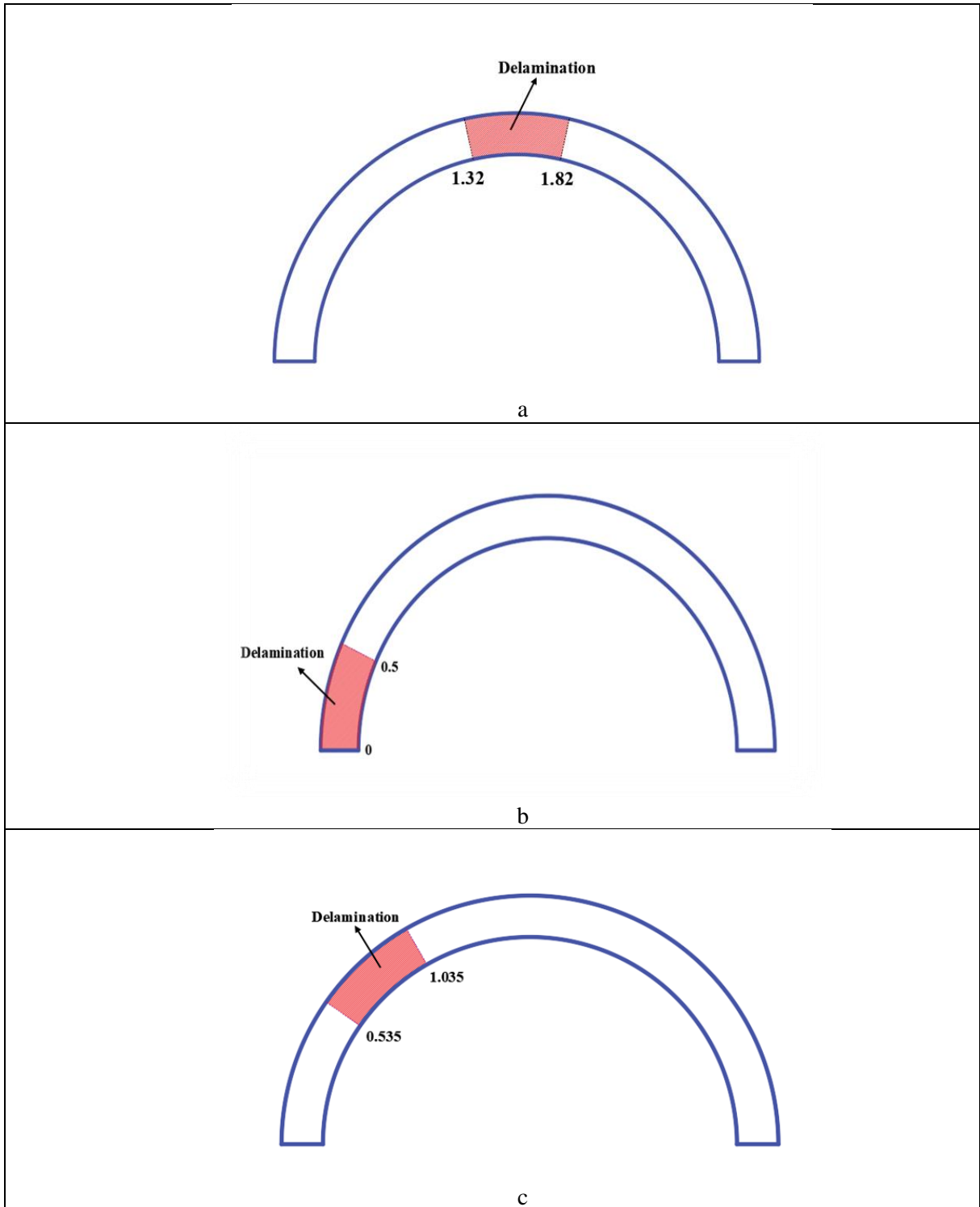
Figure 4.1.2 The location of delamination for analyzed specimen a) Center delamination (Specimen 1) b) Left end delamination (Specimen 2) c) Middle left delamination (Specimen 3)

Laminated glass units exhibit nonlinear behavior, but to analyze different aspects of linear behavior and nonlinear behavior, a comparison of nonlinear and linear approach is given in Figure 4.1.3 for a simply supported delaminated glass beam (Specimen 1). Nonlinear

and linear values are plotted as normalized deflection versus load. Normalized deflection defined as the ratio of the maximum deflection to the thickness of the glass beam. Dissociation between the linear and nonlinear results starts when normalized deflection is about 2. In Figure 4.1.3, at the P = 2 kN load level, the normalized deflection, that is, the nonlinearity level, is 13.1. It is velar from the figure that linear approach gives 1.8 times greater results than nonlinear results for 2 kN load.
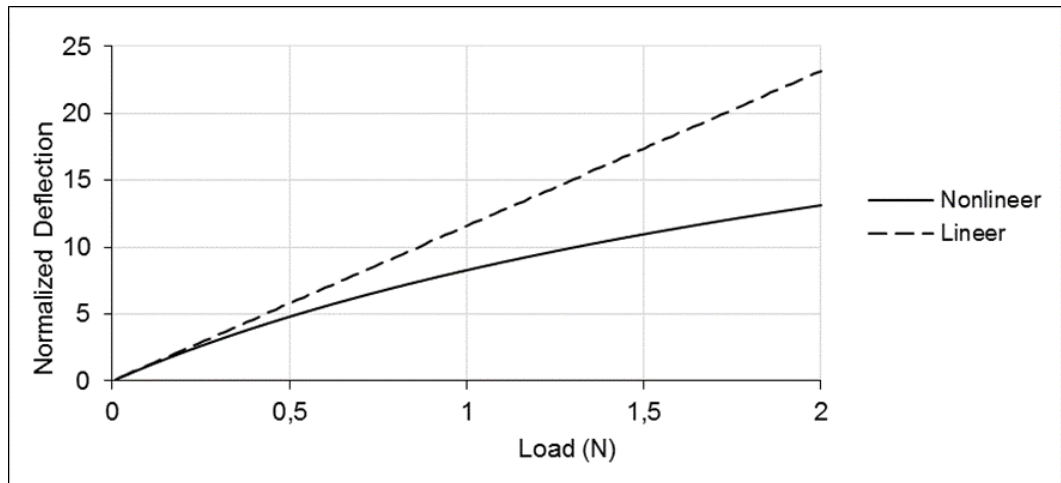
Figure 4.1.3 Load versus normalized maximum deflection ($\frac{w_{max}}{h}$) for Specimen 1 with simply supports.

Figure 4.1.4 is plotted to show the maximum displacements of different delamination states and different glass types under varying loading. Behavior of layered, monolithic and laminated glass arches are compared with the behavior of laminated glass arches with initial delaminations, at different locations. It has been observed that layered glass undergoes more deflection than other glasses and the least deflected glass type is monolithic glass. Deflection values of delaminated glass units are between those of laminated and layered units. Specimen 1's, deflection is more than other specimens. Deflection values of specimen 2 and specimen 3 are quite close to each other but deflection of specimen 3 is slightly higher than that of specimen 2.
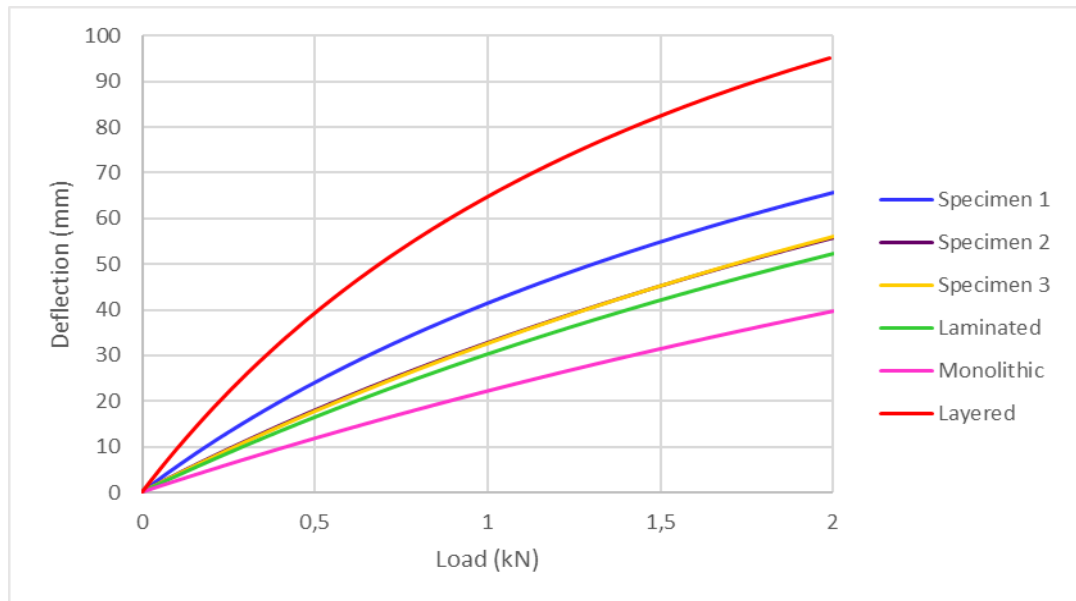
Figure 4.1.4 Maximum displacement versus load for 0.5 m delamination in different location and different glass types.

Figure 4.1.5 shows the maximum stress versus load graph for different glass types and delamination locations. When looking at the graph, layered glass has the highest stress value and monolithic has the least stress. Specimen 1 has the highest stress after layered glass. Specimen 3, Specimen 2, and laminated glass have approximately the same stress values. The stress behavior of Specimen 1 is more similar to the behavior of the laminated glass unit than the behavior of the other delaminated units.
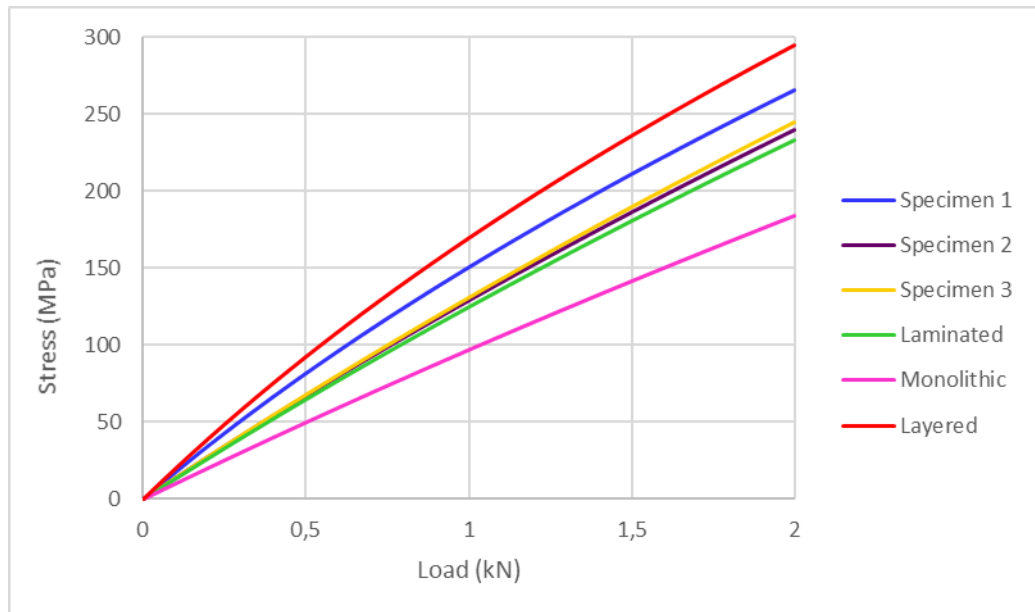
Figure 4.1.5 Maximum stresses versus load simply supported curved beams

Figure 4.1.6 and Figure 4.1.7 shows circumferential displacement of upper and lower glass unit along the curved beam length of the laminated glass curved beams for applied 2.0 kN load respectively. It is observed from Figures 4.1.6 and 4.1.7 that the circumferential deflection at the center and ends of the arch are zero due to the boundary and symmetry conditions. From figures it is observed that circumferential deflection values are positive on the left side of the beam while they are negative on the right side. In specimen 2 and specimen 3, the transition to the negative zone start on the right side of the beam. Looking at Figure 4.1.6 and 4.1.7, the circumferential displacement value change their sign between 0-0.5 meters and turn from negative to positive. For all glasses between 1.5-2 meters, the graph change direction again and go from positive to negative. Finally, between 2.5-3 meters, they take the value zero by switching from negative to positive. Comparison of radial deflections for different glass units along the arch length are presented in Figure 4.1.8. As can be seen from figure radial deflections are maximum at the midpoint of the glass arch. Radial deflection values of laminated and initially delaminated glass arches are limited by those of layered and monolithic glass arches. Due to supports, radial deflections are equal to zero at the end of the beam. Along the arch length they change their signs two times. As delamination moving through the center of the arch, the maximum value of radial deflection increases. Maximum radial deflection of layered glass beam is 2.22 times of deflection of laminated glass unit while it is 1.63 times of Specimen 1.

34
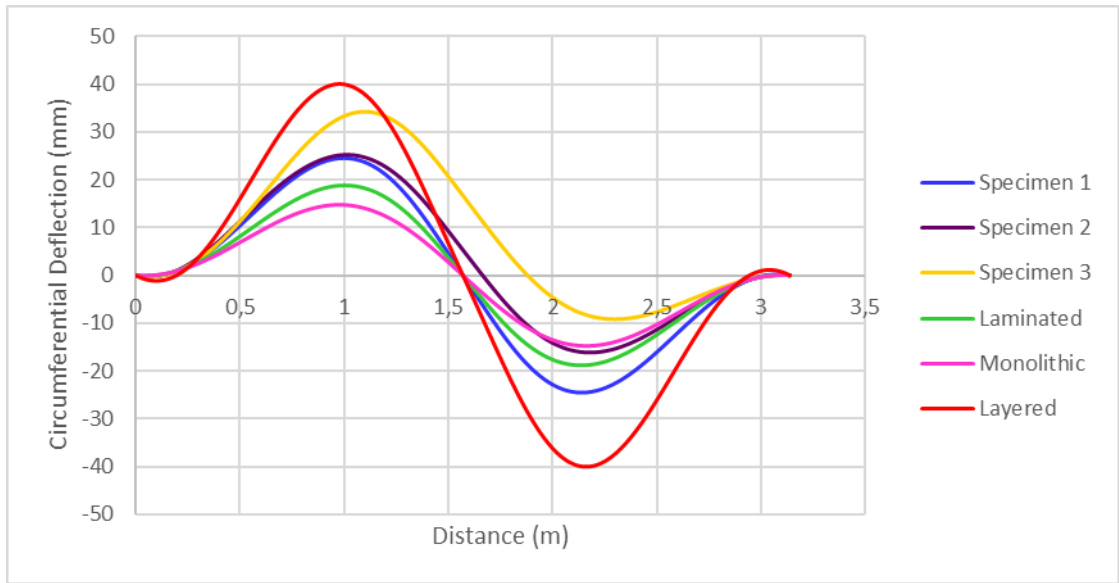
Figure 4.1.6 Circumferential displacement (u1) along the arch length for applied 2.0 kN load
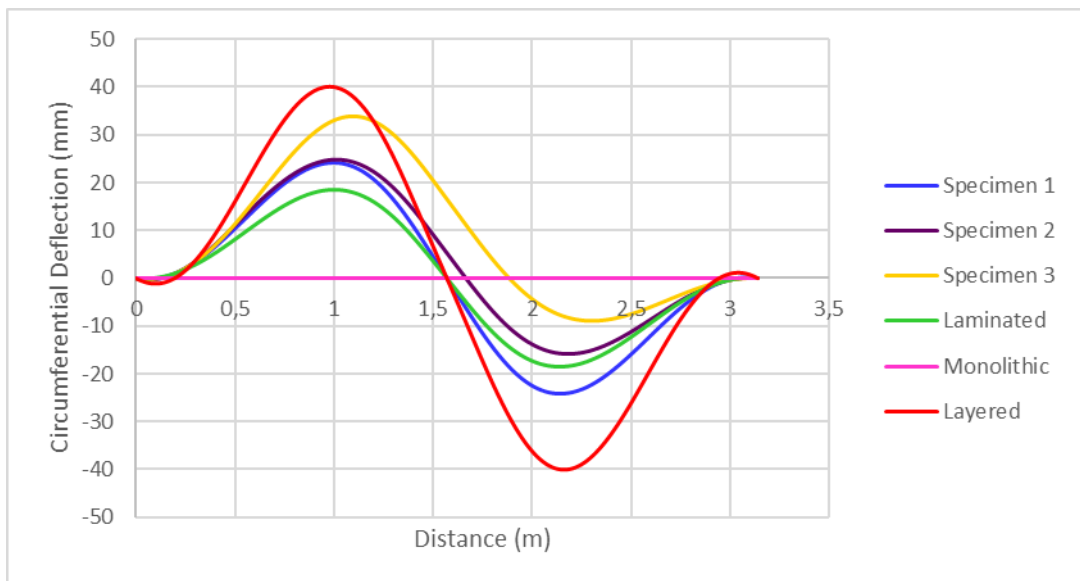
Figure 4.1.7 Circumferential deflection (u2) along the arch length for applied 2.0 kN load.
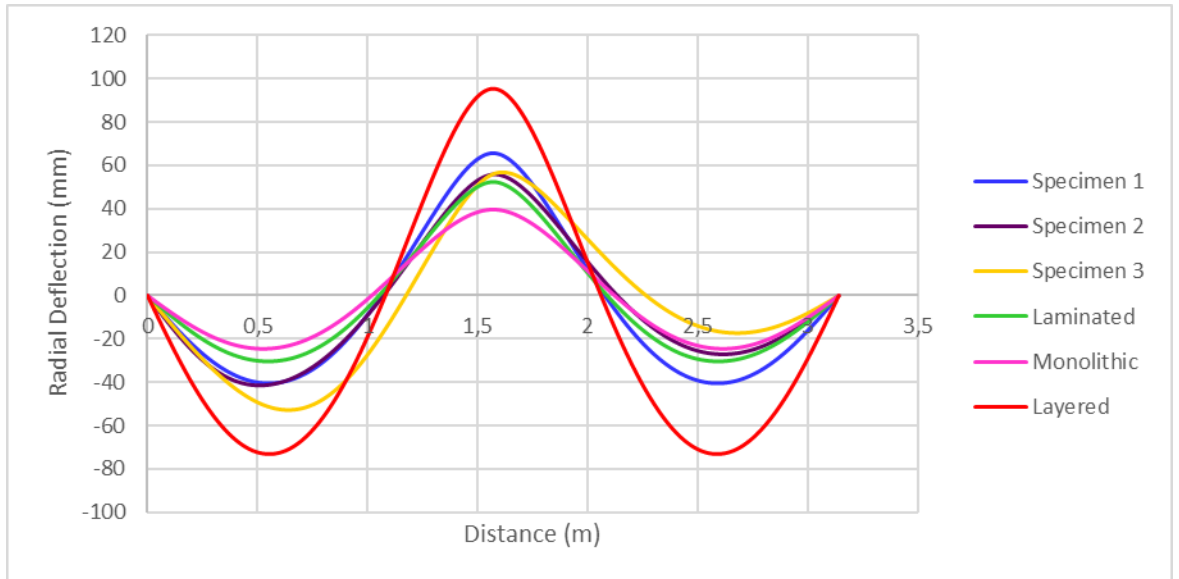
Figure 4.1.8 Radial deflections along the arch length for applied 2.0 kN load

Figure 4.1.9 is plotted to compare the radial displacements of specimen 1 for different load values. Maximum radial deflection is observed at the midpoint of the beam. As the load is increasing linearly, the distance between deflection lines decreases as a result of nonlinear behavior.
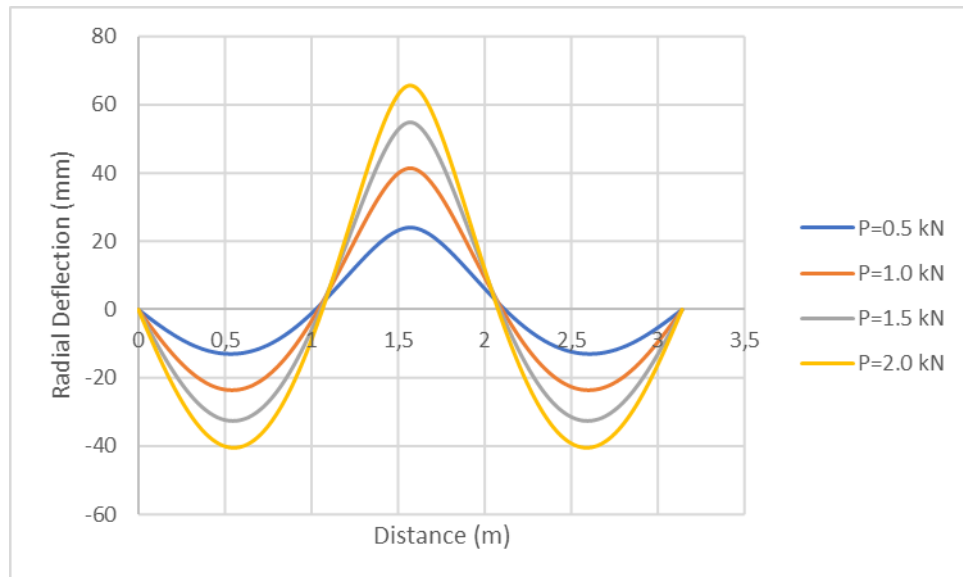
Figure 4.1.9 Radial deflections along arch length of Specimen 1.

36

The shear strain in the laminated glass unit is transferred by the PVB interlayer. The second term in Equations 3.5 and 3.6 represent the shear strain distribution between the glass plies and interlayer. Due to applied shear strain relative translation in plane direction and rotation take place in glass plies. On the top and bottom layer of unit, distributed force is transferred in the opposite directions as a result of shear strain of interlayer. Integrating Equation 3.5

$$\frac{dN_1}{d\theta} - Gbr_I\gamma_I = 0 \tag{4.1}$$

$$N_1 = \int Gbr_I\gamma(\theta)d\theta = \int G\gamma(\theta)dA = \int \tau dA \tag{4.2}$$

This equation states that, integration of shear stress along the area of layer gives the in plane force acting on the corresponding layer. Shear stress distribution along the arch length of Specimen 1 is plotted in Figure 4.1.10 for different loads. As seen in the figure, the shear stresses take the maximum values at the supports. Since there is delamination in the middle part of the beam, the shear stress takes zero value between 1.32 and 1.82 meters. Shear stresses changed sign about every quarter of the curved beam's length. The maximum shear stress occurred at the unit supports and its value is approximately 900 kPa.
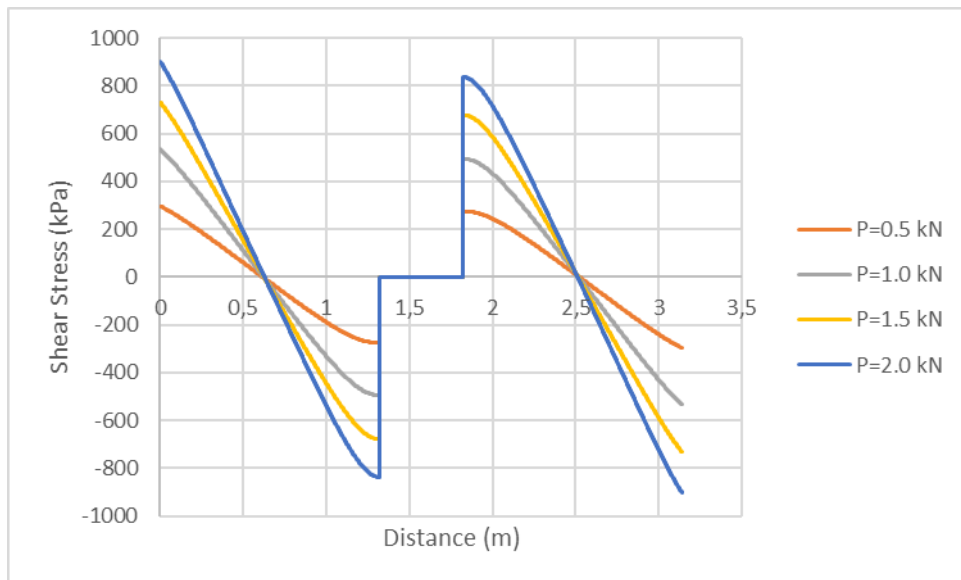
Figure 4.1.10 Variation of shear stress along the curved beam length of the Specimen 1.

Using the membrane and bending stress definitions given in the below, bending and membrane stresses on the outer and inner surface of upper and lower glass layers are given separately in Figures 4.1.11-4.1.14.

$$\sigma_{bend} = \frac{M}{I}\frac{h_i}{2} \qquad i = 1,2 \qquad\qquad (4.3)$$

$$\sigma_{mem} = \frac{N_i}{A_i} \qquad i = 1,2 \qquad\qquad (4.4)$$

While membrane stresses of upper glass unit are negative they are positive for lower glass unit. The bending stresses on upper surface of units are tension as they are compression on lower surfaces of units. Figures show that bending stress is greater than the membrane stress.
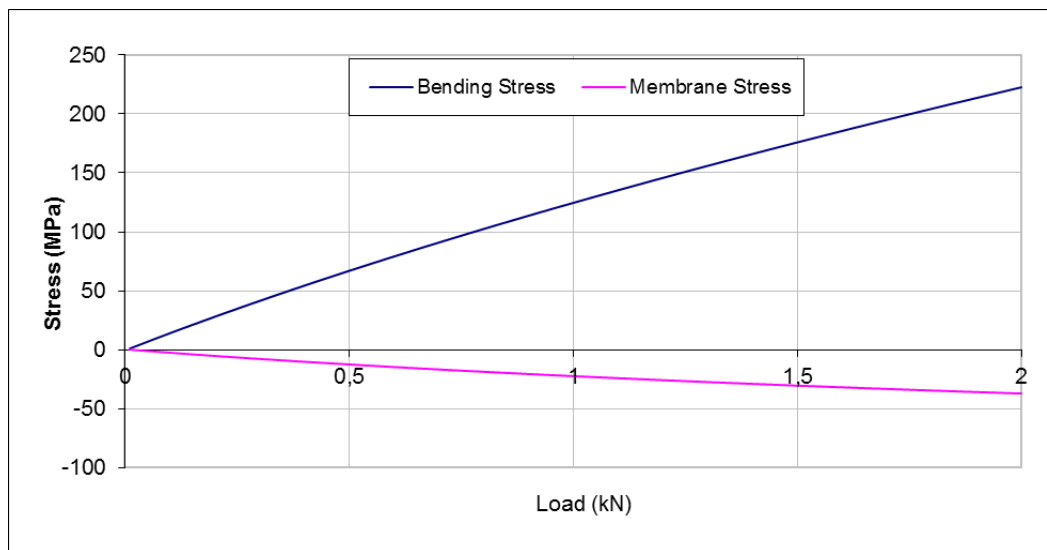
Figure 4.1.11 Membrane and bending stress of Specimen 1 for the upper surface of upper ply
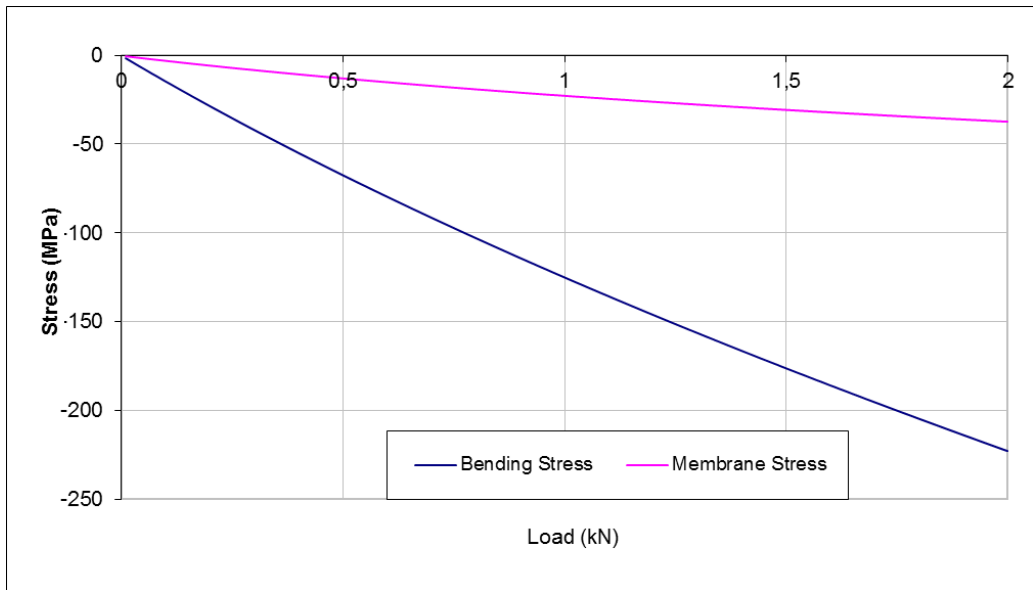
Figure 4.1.12 Membrane and bending stresses of Specimen 1for the lower surface of upper ply
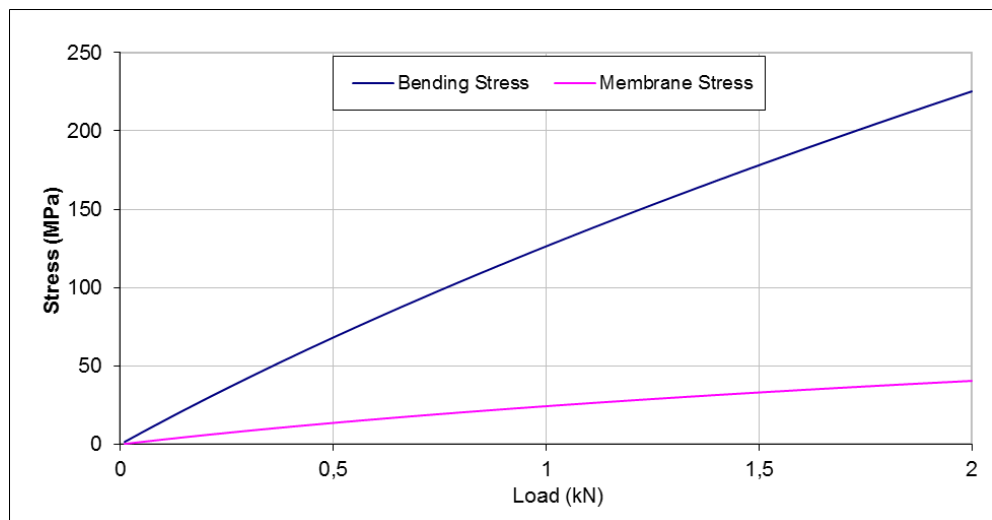
Figure 4.1.13 Membrane and bending stresses at the center of Specimen 1 for the upper surface of lower ply.
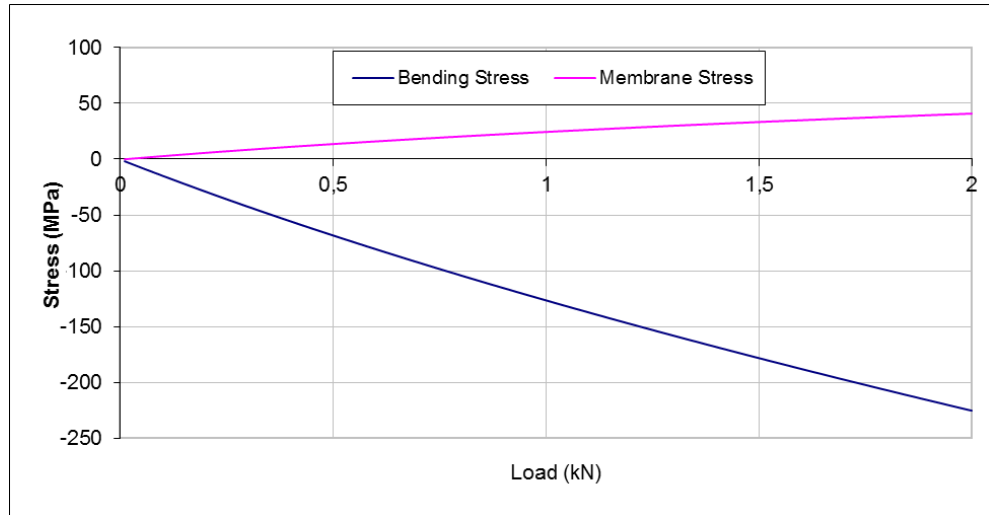
Figure 4.1.14 Membrane and bending stresses of Specimen 1 for the lower surface of the lower ply.

Combining the bending and membrane stresses of glass layers the stress acting on each surface of laminated unit can be calculated as:

$$\sigma_1^{upper} = \frac{M}{I}\frac{h_1}{2} + \frac{N_1}{A_1} \qquad (4.5)$$

$$\sigma_1^{lower} = -\frac{M}{I}\frac{h_1}{2} + \frac{N_1}{A_1} \qquad (4.6)$$

$$\sigma_2^{upper} = \frac{M}{I}\frac{h_2}{2} + \frac{N_2}{A_2} \qquad (4.7)$$

$$\sigma_1^{lower} = -\frac{M}{I}\frac{h_2}{2} + \frac{N_2}{A_2} \qquad (4.8)$$

Figure 4.1.15-4.1.18 shows the values taken by the maximum stress of Specimen 1 along the θ direction under applied different load values. Compression zones were observed on the upper surface of both the upper and lower glass as seen in Figures 4.1.15 and 4.1.17. The compressive stress on the upper surface of the glass unit against a 2kN load was observed as 260 MPa. Maximum tensile stress was observed on the lower surface of the lower and upper glass as seen in Figures 4.1.16 and 4.1.18. The maximum tension stress value obtained on the lower surface of the glass when a load of 2 kN is applied is 260 MPa. Since there is a

perfective connection between the interlayer and glass layers, the stresses on the connected surfaces of glass and interlayer are equal to each other. Sign of maximum stresses changes at two points on the domain. As can be observed from the figures the boundary stresses of the curved unit are different than zero this is result of membrane stresses.
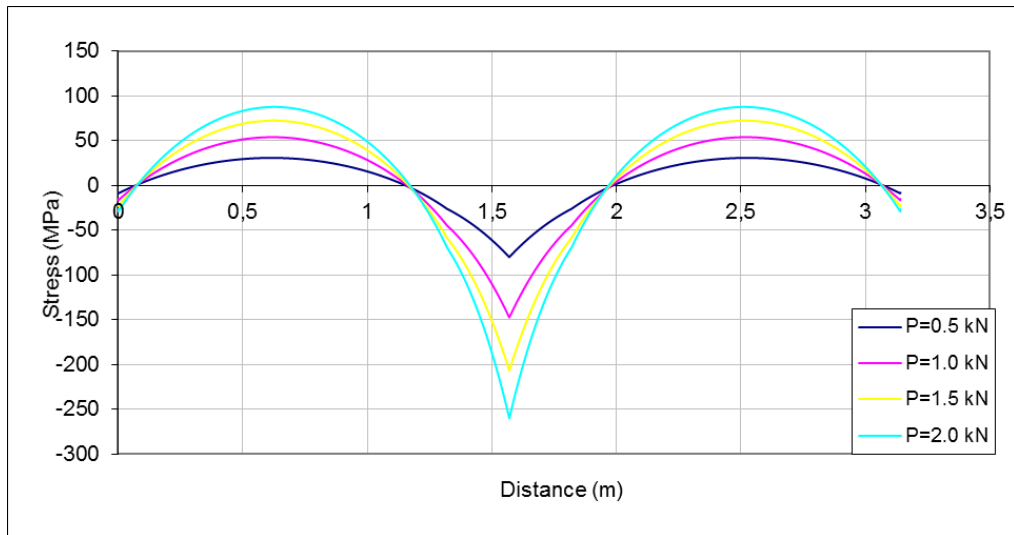
Figure 4.1.15 Stresses of Specimen 1 on the upper surface of the upper glass along the curved beam length of the simply supported beam.
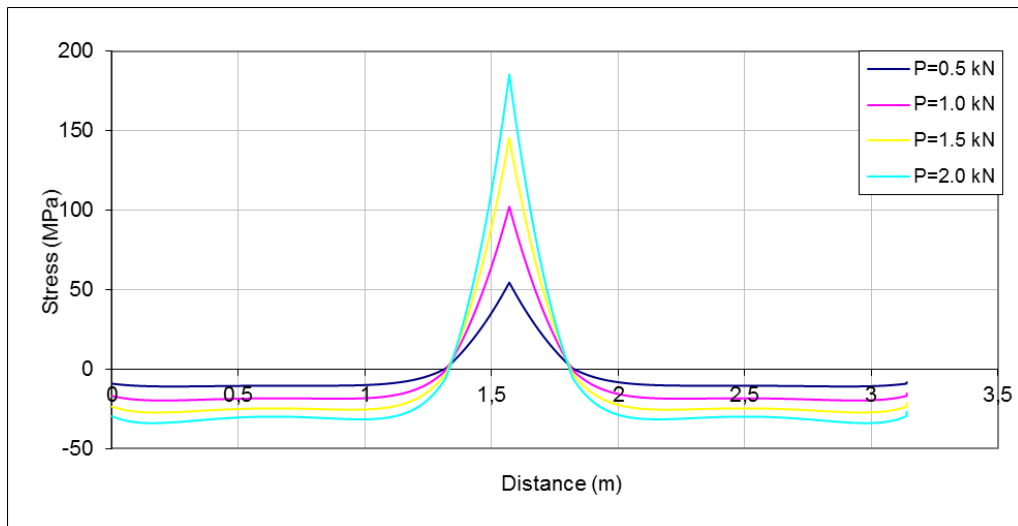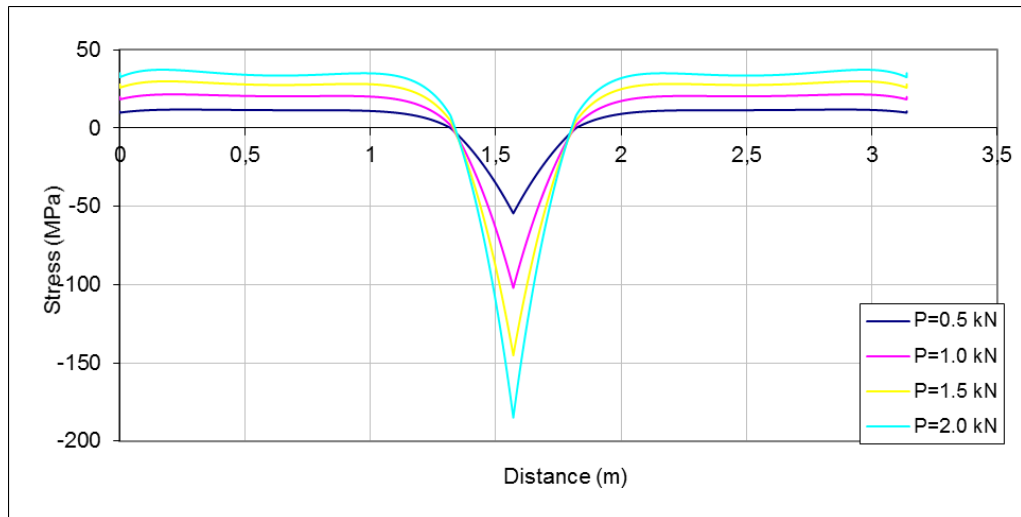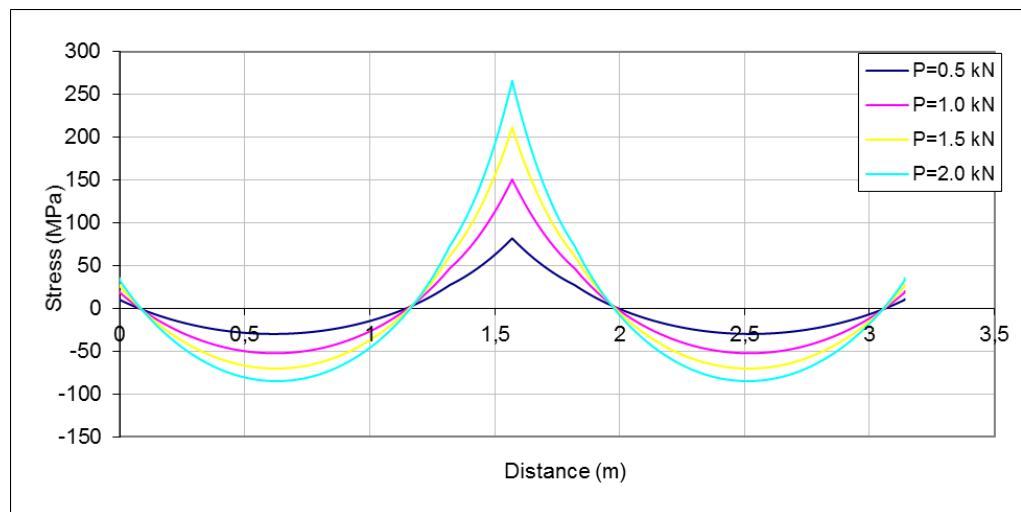

Figure 4.1.16 Stresses of Specimen 1 on the lower surface of the upper glass along the curved beam length of the simply supported beam.

Figure 4.1.17 Stresses of Specimen 1 on the upper surface of the lower glass along the curved beam length of the simply supported beam.

Figure 4.1.18 Stresses of Specimen 1 on the lower surface of the lower glass along the curved beam length of the simply supported beam.

The ratio of the maximum principal stress of monolithic glass to the maximum principal stress of laminated glass gives the strength factor. The strength factor is a major factor in determining the behavioral limits of laminated glass. Strength factor analyzes provides information about the limits laminated glass behavior. In order to say that the pressure values of monolithic glass and laminated glass are similar, the strength factor must be equal to 1.0 and the PVB interlayer must be strong enough to transfer the entire shear.

42

As seen in Figures 4.1.19-4.1.22 strength factor of Specimen 1 is nearly 0.69, while it is nearly 0.77, 0.75 and 0.79 for, Specimen 2, Specimen 3 and laminated glass, respectively.
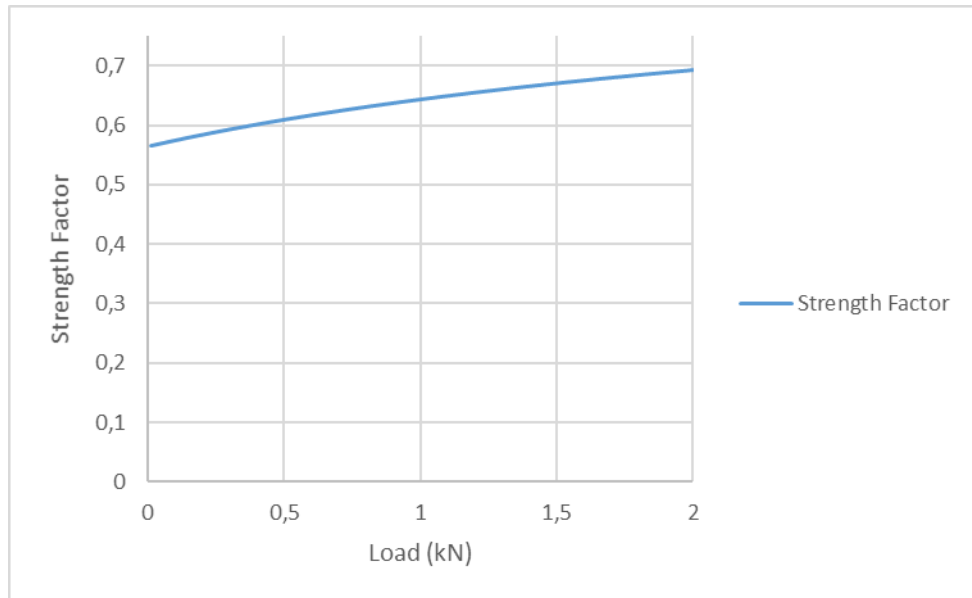
Figure 4.1.19 Change of strength factor of simply supported Specimen 1.
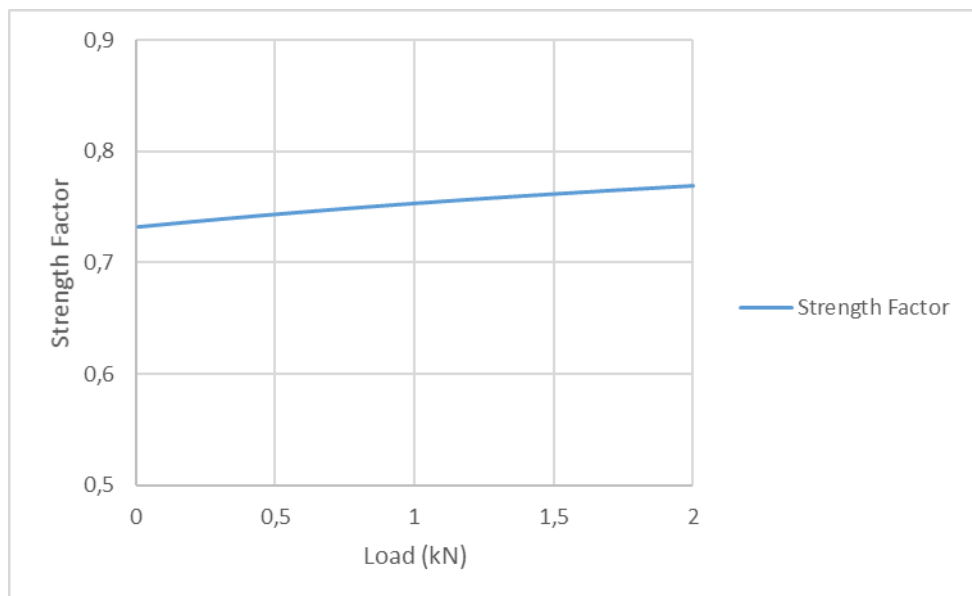
Figure 4.1.20 Change of strength factor of simply supported Specimen 2.
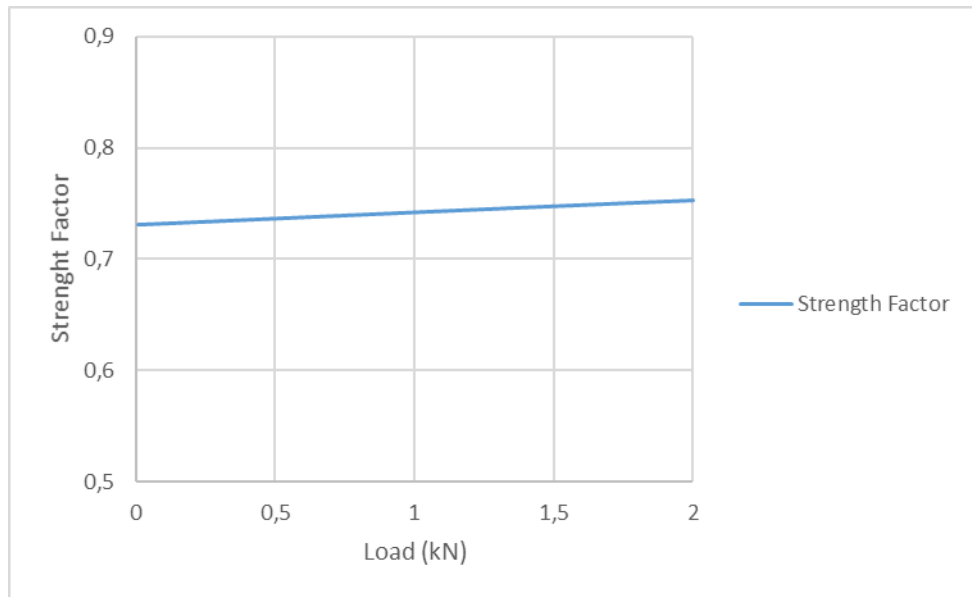
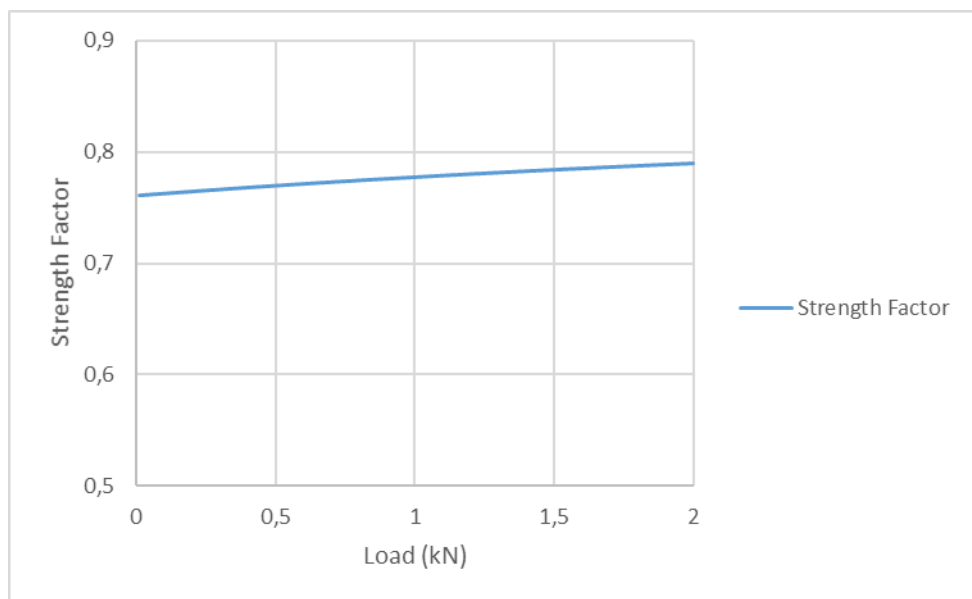Figure 4.1.21 Change of strength factor of simply supported Specimen 3.

Figure 4.1.22 Change of strength factor of simply supported laminated glass.

4.2 Curved laminated glass beam subjected to fixed supported boundary condition

Due to the restraints in horizontal direction imposed by the supports, at large deformation membrane stresses develop for fixed supported beam and they show nonlinear behavior. Mechanical behavior of this case gets more complicated due to the membrane

stresses. Also, nonlinear behavior effects the axial stiffening and cause transformation and limitation of relative movement.

Boundary conditions for the fixed support beam are as shown in Figure 4.2.1.

At $\theta = \theta_1$ and $\theta = \theta_2$ (at the supports): $\qquad w = 0 \quad$ and $\quad \dfrac{dw}{dx} = 0$

$$u_1 = 0 \text{ and } u_2 = 0$$

w=0
u1=0 $\quad \dfrac{dw}{d\theta} = 0$
u2=0

w=0
u1=0 $\quad \dfrac{dw}{d\theta} = 0$
u2=0
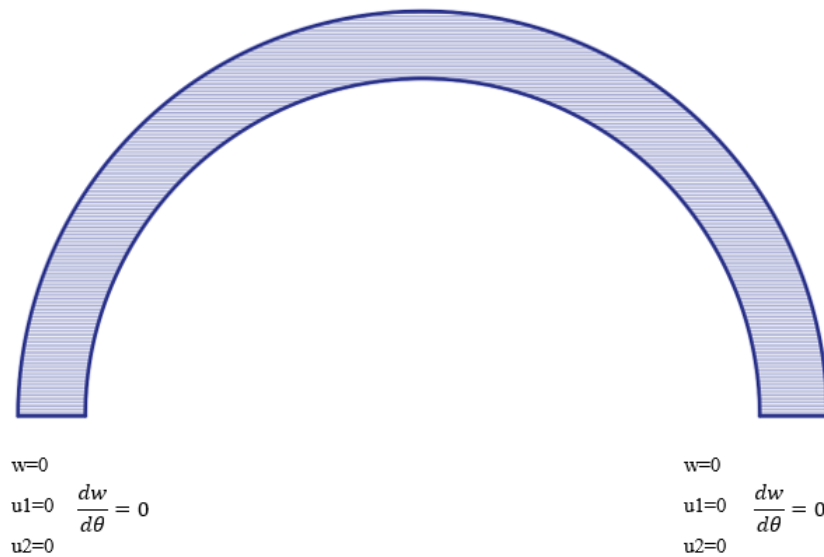
Figure 4.2.1 Representation of the boundary conditions of a fixed supported curved beam on the figure.

The same delamination conditions were applied for fix supported beams and their behavior was compared with other types of glass. Figure 4.2.2 shows normalized deflection versus load distribution. From figure it is observed that when the normalized deflection is 1.85, the nonlinear solution should be applied. Normalized deflection value is obtained as 8.97 at applied 2 kN load value. For applied 2 kN load, the normalized deflection value obtained from the linear approach is approximately 1.35 times greater than the value obtained from the nonlinear approach.
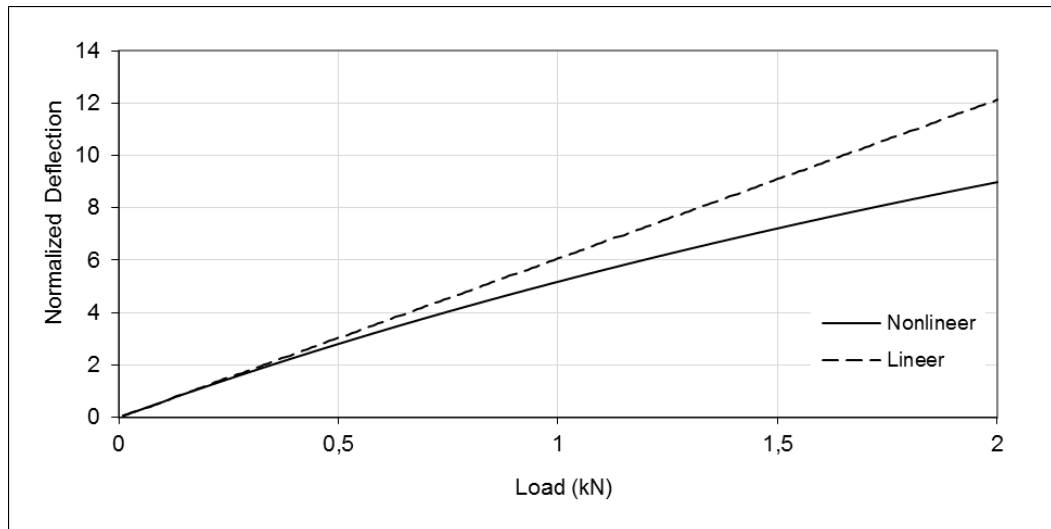
Figure 4.2.2 Load versus normalized maximum deflection ($\frac{w_{max}}{h}$) for Specimen 1 with fixed supports.

Figures 4.2.3- 4.2.4, give information about the behavior of different glass types and different delamination locations. In Figure 4.2.3, it has been observed that the layered glass has the highest deflection. And the least deflection has been observed in the monolithic glass and the deflection values of delaminated units moved between these two values. It is observed from the figure that deflection of delaminated units maybe increases or decrease with respect to that of laminated unit according to the location of delaminated region. As seen Figure 4.2.4 the layered glass has highest stress while the stress values of laminated unit and Specimen 1 are very close to each other. It is observed from the figure that stress of delaminated units are smaller than stress of laminated unit. For this reason, we can say that for fixed supported units' delamination causes a decrease in the stress values. Monolithic glass has the smallest stress value.
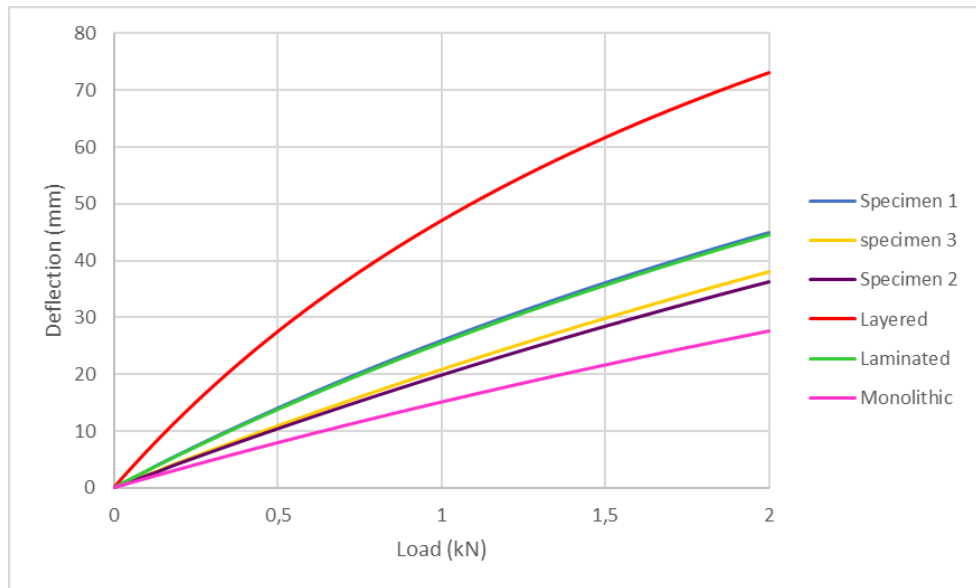
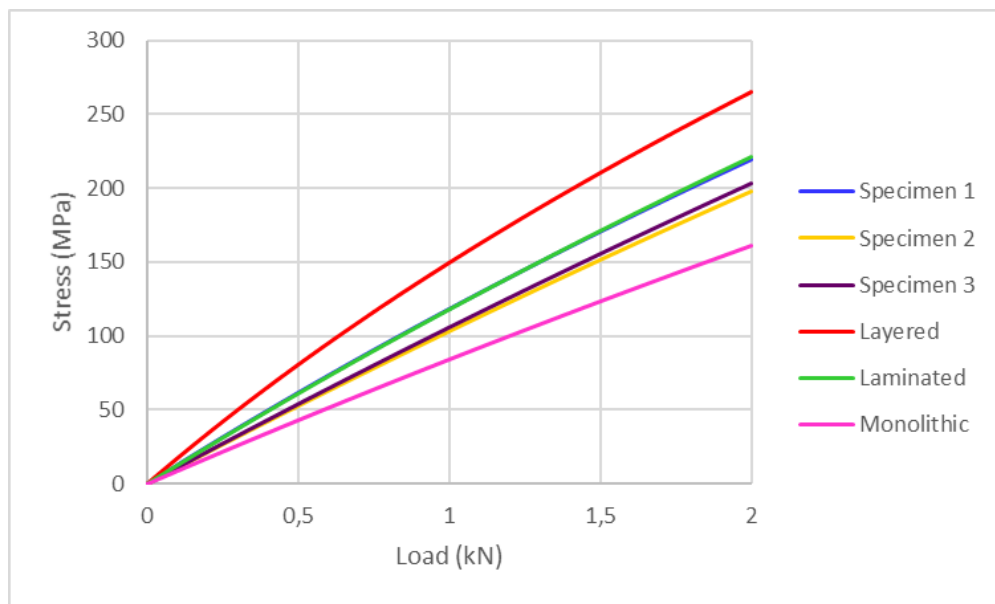Figure 4.2.3 Maximum displacement versus load for fix supported curved beams.

Figure 4.2.4 Maximum stresses versus load fix supported curved beams

Figures 4.2.5 and 4.2.6 are plotted to show the circumferential displacements of the units along arch length of the beam. It is observed that while the circumferential deflection has a positive value on the left side of the beam, it has a negative value on the right side. Layered glass has the highest circumferential deflection. Looking at the graph, it is seen that the deflection increases as the delamination gets closer to the center. Compared with Specimen 1 and laminated glass, the maximum radial deflection of the laminated glass is 1.85

47

times that of Specimen 1, while the deflection of the laminated glass unit is 1.82 times that of the Specimen 1. Figures show that while the circumferential deflection of other units are zero at the center of curved beam, for Specimen 3 that point moves to the right side of unit.
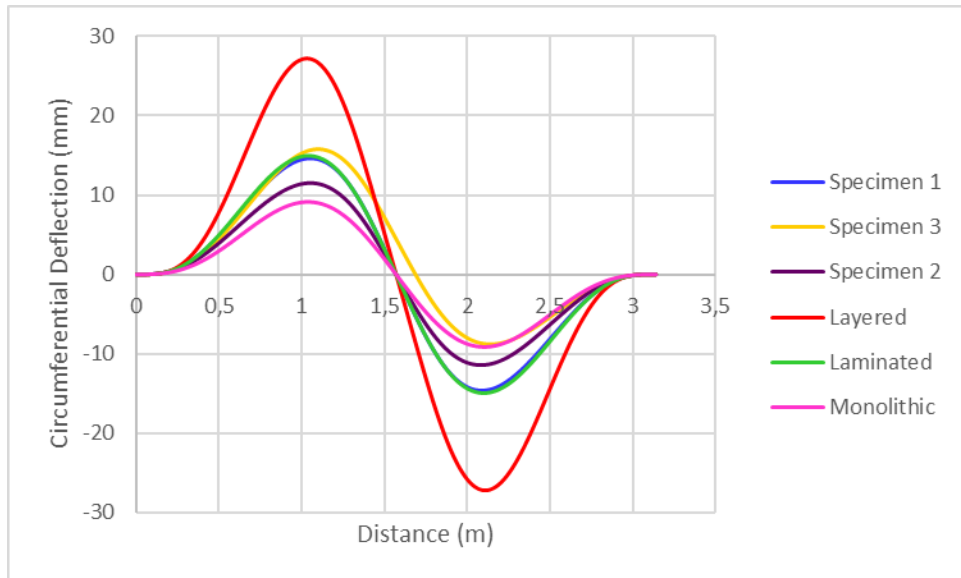
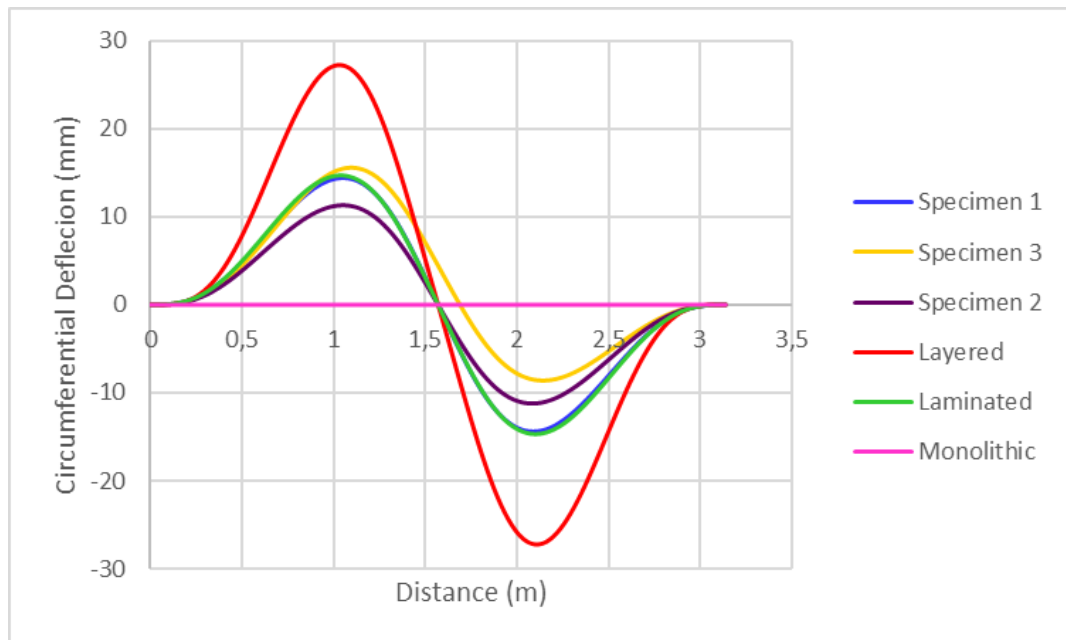Figure 4.2.5 Circumferential deflections for fixed supported beam along the curved beam length (u1) for 2.0 kN

Figure 4.2.6 Circumferential deflections for fixed supported beam (u2) along the curved beam length 2.0 kN

Figure 4.2.7 shows the radial deflections of delaminated, layered, laminated and monolithic curved glass beams when a load of 2 kN is applied. As it is seen from figure, in some regions along the arch length radial deflection value of Specimen 3 may be slightly smaller than that of monolithic unit.
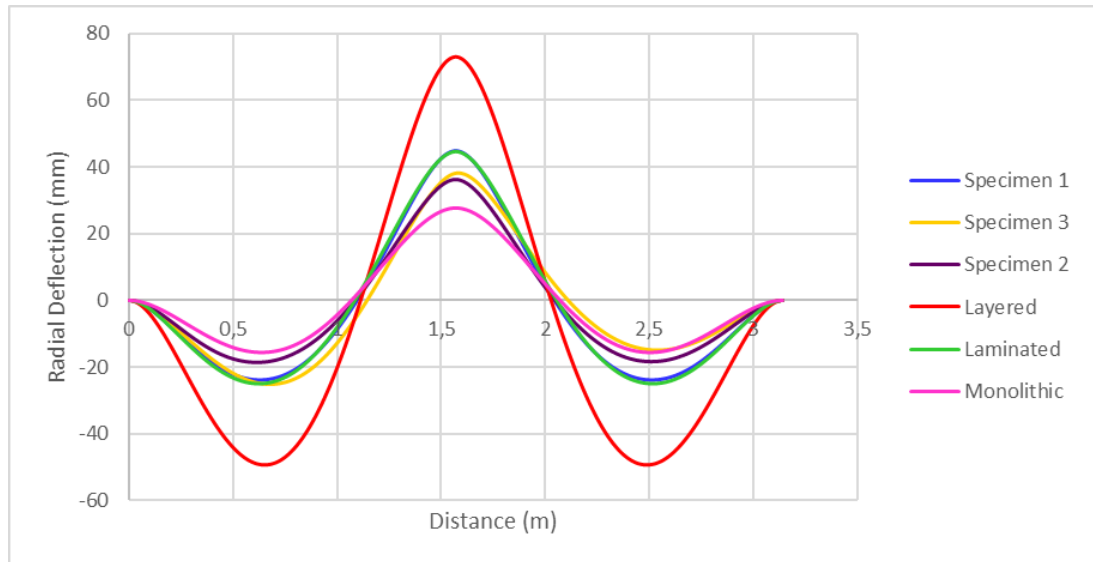
Figure 4.2.7 Radial deflections of fixed supported beam along the curved beam length for 2.0 kN

Figure 4.2.8 shows radial deflection of specimen 1 under different loads. The highest radial deflection value is observed at the midpoint of the beam. As proof of nonlinear behavior while the load is increasing linearly, the distance between deflection lines decreases. Maximum radial deflection observed at the center and for 2kN is approximately 44.84 mm.
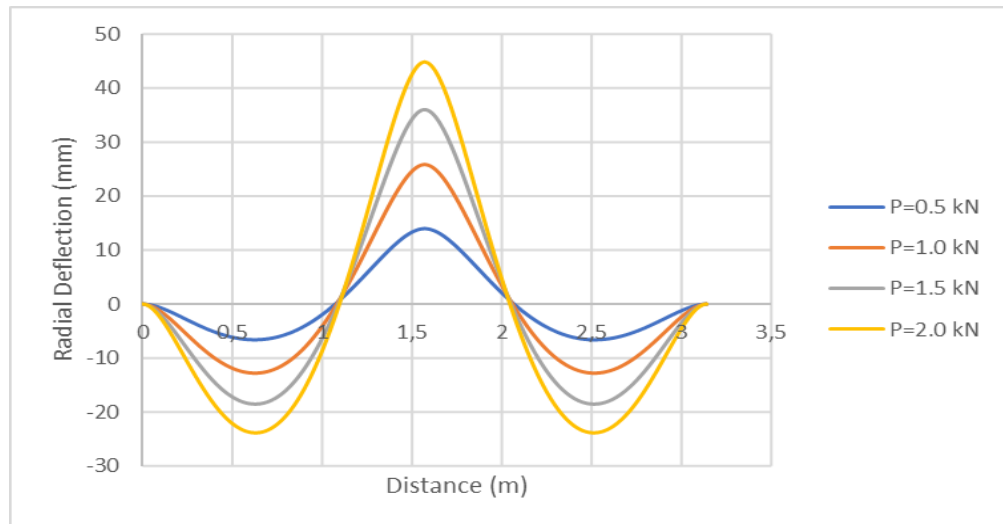
Figure 4.2.8 Radial deflections of fixed supported beam along the curved beam length of Specimen 1 for various load values.

The function of shear stress along θ direction from the left boundary to the right boundary of the delaminated fixed supported curved beam is plotted in Figure 4.2.9 for different pressure levels. Shear stresses equal zero at the delamination region and at almost every quarter of the beam. The maximum shear stress develops at the boundary of delaminated regions as nearly 665 kPa for Specimen 1.
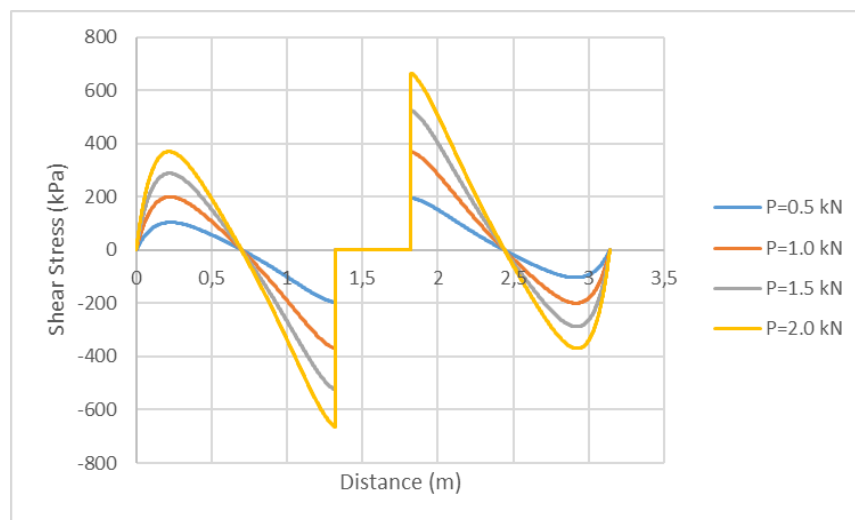
Figure 4.2.9 Variation of shear stress for fixed supported beam along the curved beam length.

In Figures 4.2.10-4.2.13, the graphs of the variation of stresses along the curved beam length on the curved beam surface for various load values are given. The maximum value of compressive stress on the upper surface of the unit is approximately 220 MPa for an applied 2 kN load. The maximum tensile stress value on the lower surface for the applied load of 2 kN is 214 MPa. The difference was observed due to the delamination condition in the glass. The stresses on the lower surface of the upper glass and the upper surface of the lower glass are equal and 167 MPa for 2 kN load.
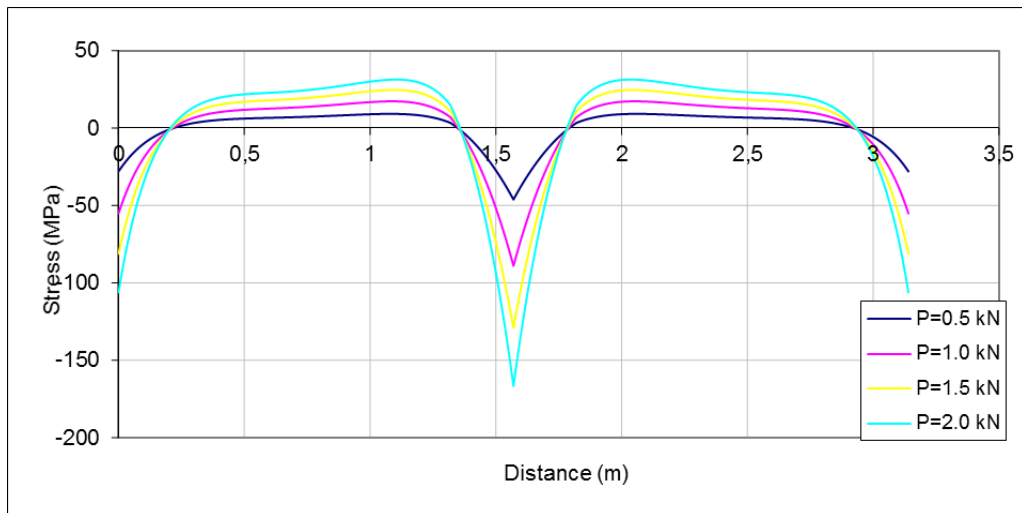
Figure 4.2.10 Stresses of Specimen 1 on the upper surface of the lower glass along the curved beam length of the fixed supported beam.
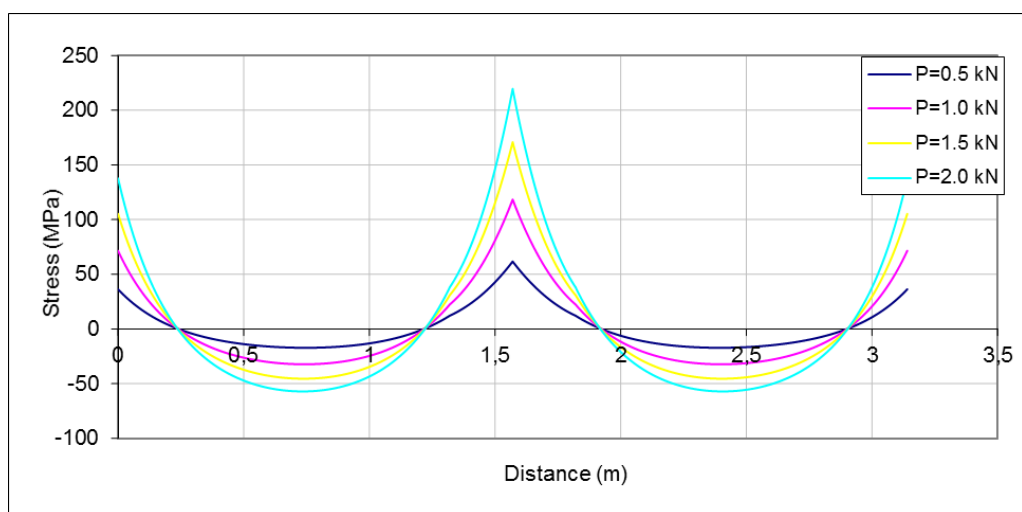

Figure 4.2.11 Stresses of Specimen 1 on the lower surface of the lower glass along the curved beam length of the fixed supported beam.
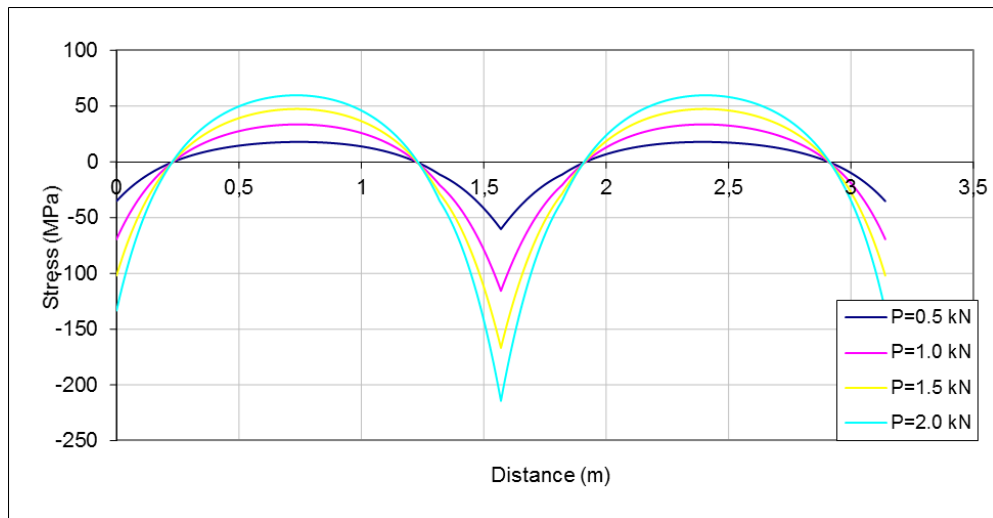
51

Figure 4.2.12 Stresses on the upper surface of the upper glass along the curved beam length of the fixed supported beam in the center of the beam
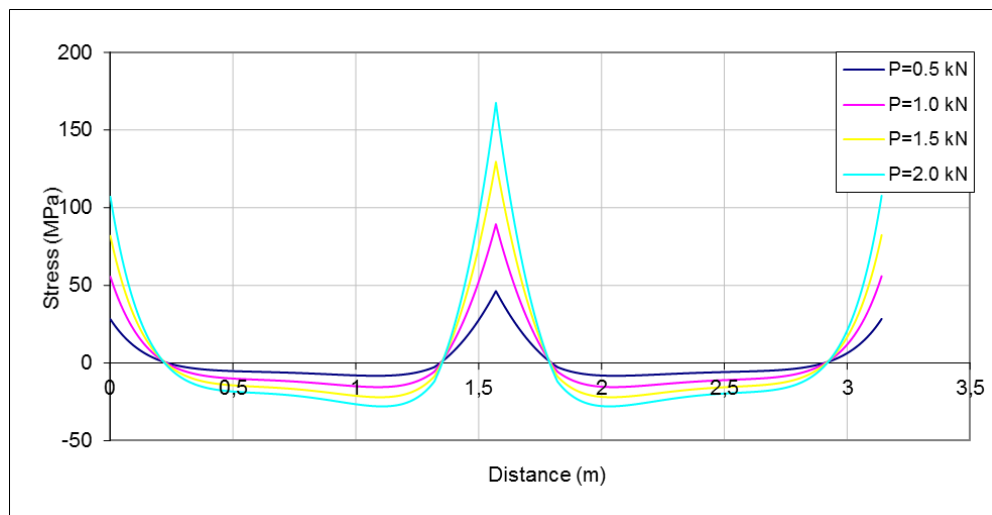

Figure 4.2.13 Stresses on the lower surface of the upper glass along the curved beam length of the fixed supported beam in the center of the beam

In Figures 4.2.14-4.2.17 laminated glass strength factor is 0.62, Specimen 1 is 0.61, Specimen 2 is 0.764 and Specimen 3 is 0.726.
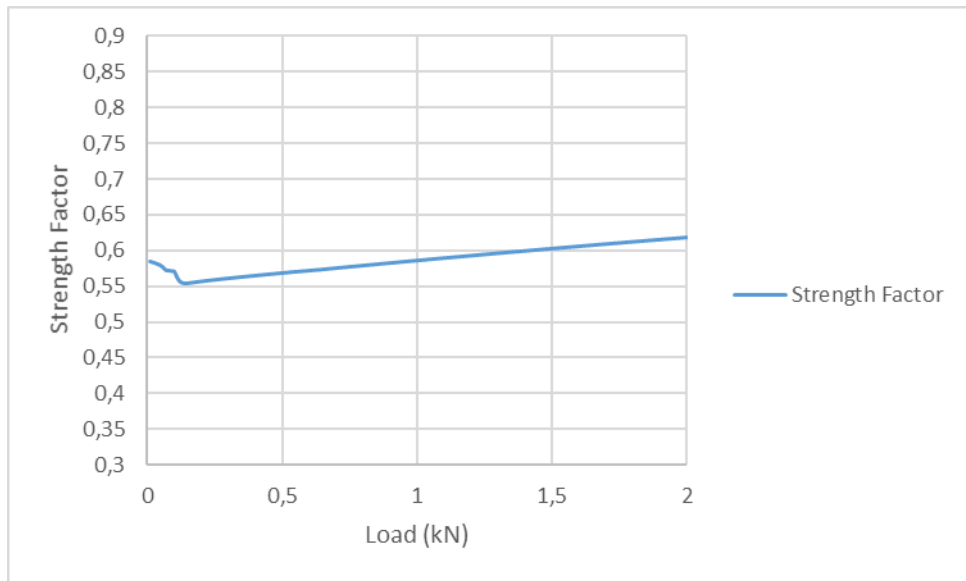
Figure 4.2.14 Change of strength factor for delaminated fixed supported Specimen 1.
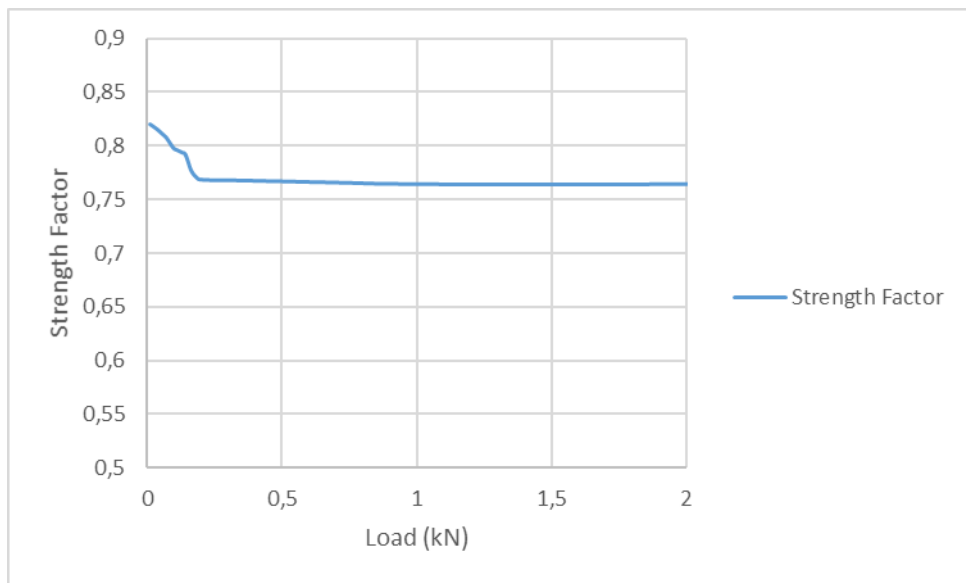

Figure 4.2.15 Change of strength factor for delaminated fixed supported Specimen 2.
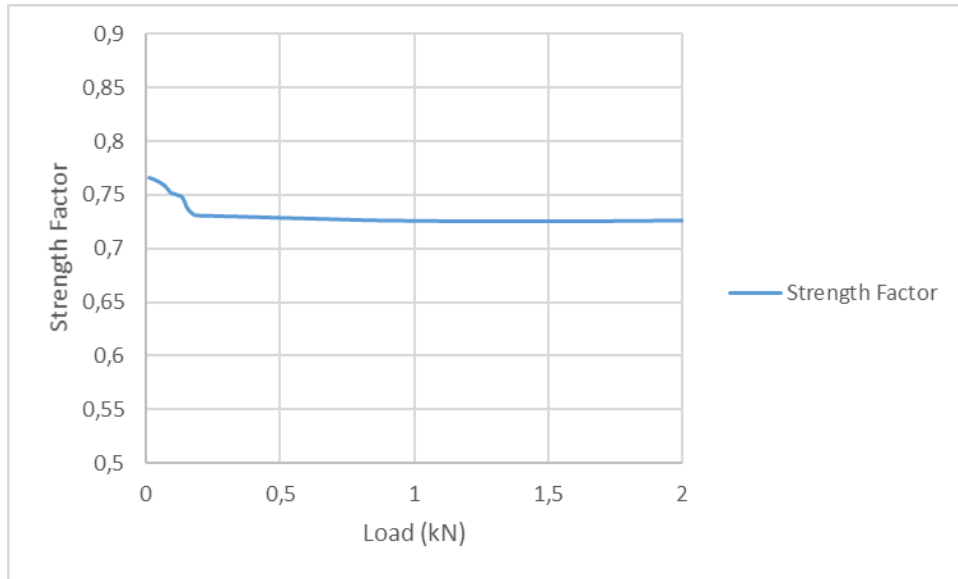
Figure 4.2.16 Change of strength factor for delaminated fixed supported Specimen 3.
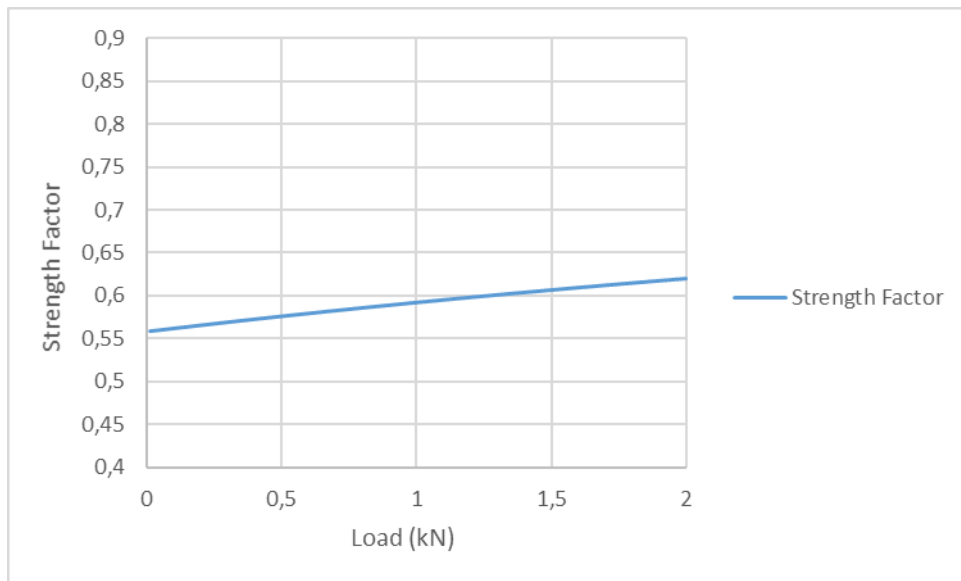

Figure 4.2.17 Change of strength factor for fixed supported laminated glass.

In order to investigate the effect of boundary conditions on the behavior of delaminated curved glass beam the results obtained for simply and fixed supported units are compared. Comparison graphs obtained according to different boundary conditions of curved laminated glass beam are given below. The comparison of deflection values and their maximum values are given in Figure 4.2.18. According to this graph, the deflection of the simply supported beam is higher than the fixed support beam. The comparison of stress values is given in

54

Figure 4.2.19. According to this graph, the stress value of the simply support beam is higher than the fixed support beam.
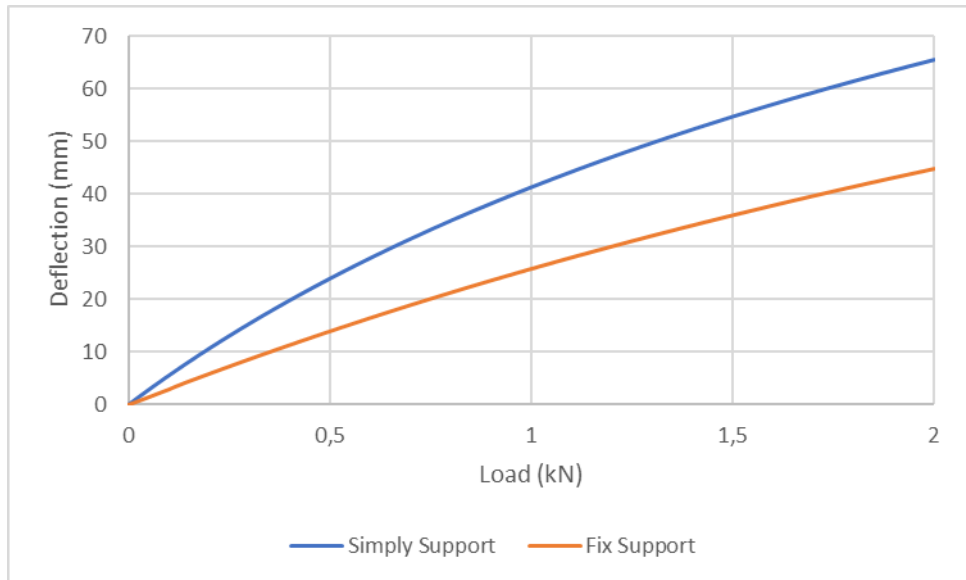

Figure 4.2.18 Comparison of maximum displacements for simply and fixed boundary conditions
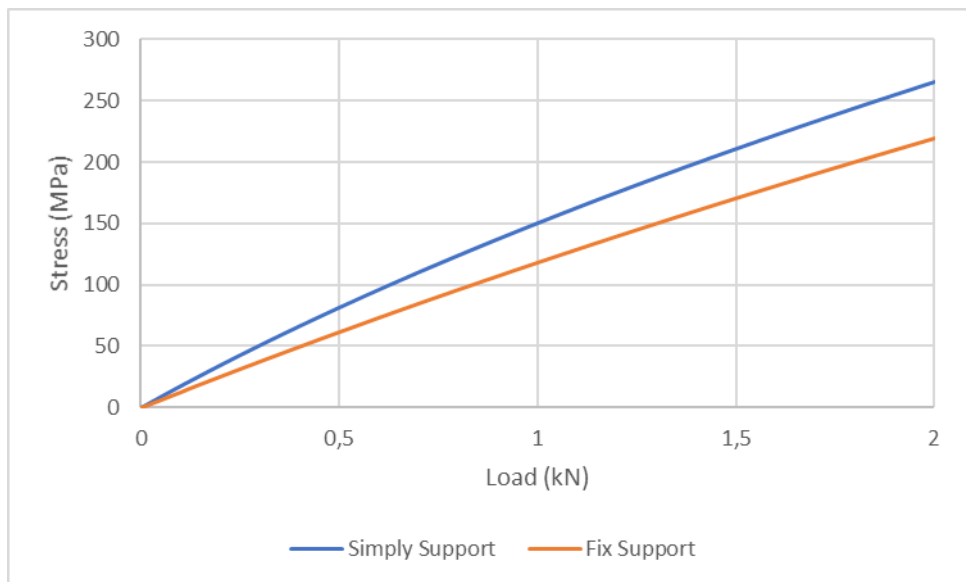

Figure 4.2.19 Comparison of maximum stresses for simply and fixed boundary conditions.

Comparison of radial deflection and surface stresses of curved beam for simple support and fixed supported boundary conditions along the arc length under 2 kN load are given in Figures 4.2.20 and 4.2.21, respectively.
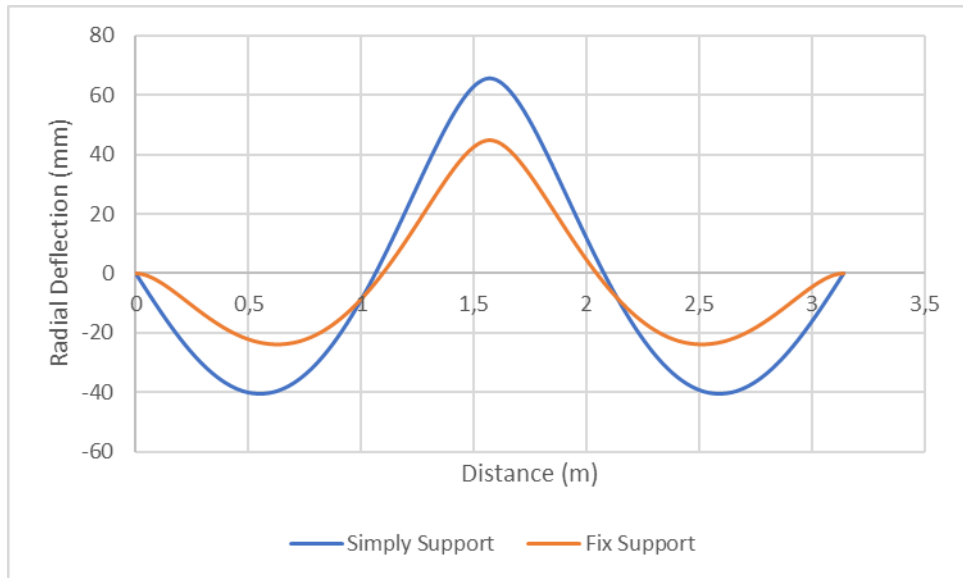

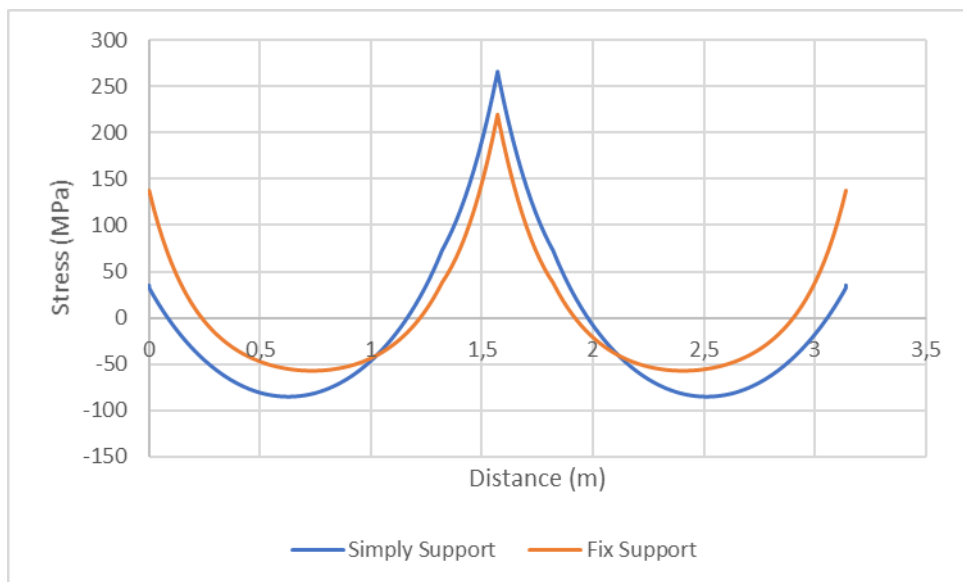Figure 4.2.20 Comparison of radial deflections along the curved beam length of the beam

Figure 4.2.21 Comparison of maximum stresses on the upper surface of the upper glass along the curved beam length of the beam

5. DISCUSSION

Although glass is known as a fragile material, technology of today made it a strong, durable and versatile material which can be used construction of buildings. Nowadays, with the invent of laminated glass, it is used in the building industry as a structural member.

Many studies have been done about laminated glass from past to present. These studies are mostly about the use of laminated glass in the automotive and space industry. Due to the resistance of laminated glass to dispersion in case of any explosions and impact, it is used on the windshield of cars to minimize injuries in the event of a possible accident. Therefore, the studies are mostly carried out by simulating car accidents and explosions, and it has been observed that the studies are generally experimental.

In this study, glass is considered as a building material. Especially, the lack of information in the literature about the behavior of curved laminated glass in the delamination condition has created an idea for this study and a mathematical model a has been developed for different boundary conditions. A commercial package program (Abaqus) was used to compare and control the assumptions of the developed mathematical model. With this study, the behavior of the glass in the case of delamination has been evaluated and presented from various angles according to different boundary conditions and different location of the delamination. This study shows that delamination may cause different effect on deflection and stress functions also it may cause an increase or reduction on the strength of unit according to the location of delaminated region. It is observed from the study that for simply supported unit strength of Specimen 1 gets closer to that of layered unit. Since the load is applied to the center of unit we can say that the region which the load is applied determine the behavior of beam. Deflection and stress values of simply supported Specimen 1 are greater than those of fixed supported one.

6. CONCLUSION AND RECOMMENDATION

In this thesis, nonlinear field differential equations derived by Dural (2011) and varied experimentally by Aşık et al. (2014) are modified for the curved delaminated glass beams. Variational calculus and minimum potential energy theorem are employed to obtain the field differential equations. A computer program based on the formulation has been used in the analysis and it has also been modified for the analysis of laminated curved glass units having initial delamination. Detailed knowledge is achieved regarding stress and displacement functions for curved laminated glass beam having initial delamination in different locations and is given for the use in engineering practice. The results of the mathematical model described in this study provide important information for understanding the behavior of the curved laminated glass beam with delamination. It shows that boundary conditions and location of delamination are important factors in determining the response of units. Depending on the conclusion obtained herein, it is inferred that the developed mathematical model is a convenient method to investigate behavior of delaminated and laminated glass curved beams. The effect of location of delamination, the nonlinearity level, stress and displacement functions are observed. In order to observe the effect of different boundary conditions on the behavior of the delaminated curved glass beam, the mathematical model is solved for two different boundary conditions and the results are given in graphs. A significant conclusion obtained from study states that the delaminated glass units shows nonlinear behavior. Nonlinearity level of fixed supported center delaminated curved beam is found to be higher than that of simply supported one.

To specify strength of laminated units strength factor analyze is performed and design charts are used. Strength factors are presented for delaminated and laminated glass curved beams. The results show that strength factor of the simply supported curved beam is greater than that of fixed supported unit. Strength factor of Specimen 1, which has delamination at the center of unit, is smaller than the other specimens.

The response of laminated and delaminated glass curved beams are bounded by those of monolithic and layered ones. In the graphics obtained, it was observed that layered glass took the highest value in the graphics, while the monolithic glass took the least value. Specimen 1

shows the closest behavior to layered glass. Analyses were made in different boundary conditions and as a result, it was seen that the simply supported beam had more stress and deflection values than the fixed supported beam. The location of the delaminated area can affect the strength of the laminated glass beam. One of the important results of the study is that the stress function and deflection function were affected differently in the case of delamination. The finite element model was used to check the accuracy of the assumptions of the developed model and this model showed that the assumptions were correct. When the results are compared with the program (Abaqus), it has been determined that the model design to analyze the behavior of curved laminated glass beams gives reliable results.

REFERENCES

Aşık, M. Z., and Tezcan, S. (2005). A mathematical model for the behavior of laminated glass beams. *Computer and Structures*, 83(21-22), 1742-1753.doi:10.1016/j.compstruc.2005.02.020

Aşık, M. Z., Dural, E., Yetmez, M., and Uzhan, T. (2014). A mathematical model for the behavior of laminated uniformly curved glass beams. *Composites Part B: Engineering, 58, 593–604.* doi:10.1016/j.compositesb.2013.11.004

Centelles, X., Castro, J. R., and Cabeza, L. F. (2020). Double-lap shear test on laminated glass specimens under diverse ageing conditions. *Construction and Building Materials*, 249, 118784. doi:10.1016/j.conbuildmat.2020.118784

Chen, J., Xu, J., Yao, X., Xu, X., Liu, B., and Li, Y. (2014). Different driving mechanisms of in-plane cracking on two brittle layers of laminated glass. *International Journal of Impact Engineering*, 69, 80–85. doi:10.1016/j.ijimpeng.2014.02.014

Dural E. (2011) *Analysis of laminated glass arches and cylindrical shells* Doctoral Thesis, Middle East Technical University Graduate School of Natural and Applied Sciences, Ankara

Dural, E. (2016). Analysis of delaminated glass beams subjected to different boundary conditions. *Composites Part B:Engineering*,101, 132-146

doi:10.1016/j.compositesb.2016.07.002

Gadelrab, R. M. (1996). The effect of the delamination on the natural frequencies of a laminated composite beam. *Journal of Sound and Vibration*, 197(3), 283–292.

 doi:10.1006/jsvi.1996.0532

Geleta, T. N., Woo, K., and Lee, B. (2018). Delamination Behavior of L-Shaped Laminated Composites. *International Journal of Aeronautical and Space Sciences*, 19(2), 363–374. doi:10.1007/s42405-018-0038-y

Hooper, J. A. (1973). On the bending of architectural laminated glass. *International Journal of Mechanical Sciences*, 15(4), 309–323. doi:10.1016/0020-7403(73)90012-x

Ibekwe, S. I., Mensah, P. F., Li, G., Pang, S.-S., and Stubblefield, M. A. (2007). Impact and post impact response of laminated beams at low temperatures. *Composite Structures*, 79(1), 12–17. doi:10.1016/j.compstruct.2005.11.025

Jaśkowiec, J. (2015). Numerical Modeling Mechanical Delamination in Laminated Glass by XFEM. *Procedia Engineering, 108, 293–300.* doi:10.1016/j.proeng.2015.06.150

La Saponara, V., Muliana, H., Haj-Ali, R., and Kardomateas, G. A. (2002). Experimental and numerical analysis of delamination growth in double cantilever laminated beams. *Engineering Fracture Mechanics*, 69(6), 687–699. doi:10.1016/s0013-7944(01)00106-0

Peng, Y., Yang, J., Deck, C., & Willinger, R. (2013). Finite element modeling of crash test behavior for windshield laminated glass. *International Journal of Impact Engineering*, 57, 27–35. doi:10.1016/j.ijimpeng.2013.01.010

Serafinavičius, T., Lebet, J.-P., Louter, C., Lenkimas, T., and Kuranovas, A. (2013). Long-term Laminated Glass Four Point Bending Test with PVB, EVA and SG Interlayers at Different Temperatures. *Procedia Engineering*, 57, 996–1004.

 doi:10.1016/j.proeng.2013.04.126

Zubillaga, L., Turon, A., Renart, J., Costa, J., and Linde, P. (2015). An experimental study on matrix crack induced delamination in composite laminates. *Composite Structures*, 127, 10–17. doi:10.1016/j.compstruct.2015.02.077

CURRICULUM VITAE

Last name, First name: VURAL, Simge

Nationality: T.C

Foreign Language: English

Education

Level	Institute	Date of graduation
Master's	Natural and Applied Science institute	
Bachelor's	Civil Engineering- Faculty of Engineering Muğla Sıtkı Koçman University	25/06/2019